Article

Current Biology

CB1 Receptors in the Anterior Piriform Cortex Control Odor Preference Memory

Highlights

- CB1 receptors are highly expressed in anterior piriform cortex (aPC) interneurons
- aPC-CB1 receptors control retrieval of conditioned odor preference (COP)
- aPC-CB1 receptors are not involved in retrieval of conditioned odor aversion
- COP retrieval is linked to CB1-dependent reduction of aPC inhibitory transmission

Authors

Geoffrey Terral, Arnau Busquets-Garcia, Marjorie Varilh, ..., Pedro Grandes, Guillaume Ferreira, Giovanni Marsicano

Correspondence

guillaume.ferreira@inra.fr (G.F.), giovanni.marsicano@inserm.fr (G.M.)

In Brief

Terral et al. explore the role of the endocannabinoid system in olfactory memory functions. They show that cannabinoid type-1 (CB1) receptors control the retrieval of appetitive, but not aversive, olfactory memory, associated with a modulation of local inhibitory transmission onto specific principal neurons of the anterior piriform cortex.

Terral et al., 2019, Current Biology *29*, 2455–2464
August 5, 2019
https://doi.org/10.1016/j.cub.2019.06.041

CellPress

Current Biology
Article

CB1 Receptors in the Anterior Piriform Cortex Control Odor Preference Memory

Geoffrey Terral,[1,2] Arnau Busquets-Garcia,[1,2] Marjorie Varilh,[1,2] Svein Achicallende,[3,4] Astrid Cannich,[1,2] Luigi Bellocchio,[1,2] Itziar Bonilla-Del Río,[3,4] Federico Massa,[1,2] Nagore Puente,[3,4] Edgar Soria-Gomez,[1,2,3,4,5] Pedro Grandes,[3,4] Guillaume Ferreira,[2,6,7,*] and Giovanni Marsicano[1,2,7,8,*]
[1]INSERM, U1215 NeuroCentre Magendie, 146 rue Léo Saignat, 33077 Bordeaux Cedex, France
[2]University of Bordeaux, 146 rue Léo Saignat, 33000 Bordeaux, France
[3]Department of Neurosciences, University of the Basque Country UPV/EHU, Barrio Sarriena s\n, 48940 Leioa, Spain
[4]Achucarro Basque Center for Neuroscience, Science Park of the UPV/EHU, 48940 Leioa, Spain
[5]IKERBASQUE, Basque Foundation for Science, Maria Diaz de Haro 3, 48013 Bilbao, Spain
[6]INRA, Bordeaux INP, Nutrition and Integrative Neurobiology, UMR 1286, 146 rue Léo Saignat, 33076 Bordeaux Cedex, France
[7]Senior author
[8]Lead Contact
*Correspondence: guillaume.ferreira@inra.fr (G.F.), giovanni.marsicano@inserm.fr (G.M.)
https://doi.org/10.1016/j.cub.2019.06.041

SUMMARY

The retrieval of odor-related memories shapes animal behavior. The anterior piriform cortex (aPC) is the largest part of the olfactory cortex, and it plays important roles in olfactory processing and memory. However, it is still unclear whether specific cellular mechanisms in the aPC control olfactory memory, depending on the appetitive or aversive nature of the stimuli involved. Cannabinoid-type 1 (CB1) receptors are present in the aPC (aPC-CB1), but their potential impact on olfactory memory was never explored. Here, we used a combination of behavioral, genetic, anatomical, and electrophysiological approaches to characterize the functions of aPC-CB1 receptors in the regulation of appetitive and aversive olfactory memory. Pharmacological blockade or genetic deletion of aPC-CB1 receptors specifically impaired the retrieval of conditioned odor preference (COP). Interestingly, expression of conditioned odor aversion (COA) was unaffected by local CB1 receptor blockade, indicating that the role of aPC endocannabinoid signaling is selective for retrieval of appetitive memory. Anatomical investigations revealed that CB1 receptors are highly expressed on aPC GABAergic interneurons, and *ex vivo* electrophysiological recordings showed that their pharmacological activation reduces miniature inhibitory postsynaptic currents (mIPSCs) onto aPC semilunar (SL), but not pyramidal principal neurons. COP retrieval, but not COA, was associated with a specific CB1-receptor-dependent decrease of mIPSCs in SL cells. Altogether, these data indicate that aPC-CB1 receptor-dependent mechanisms physiologically control the retrieval of olfactory memory, depending on odor valence and engaging modulation of local inhibitory transmission.

INTRODUCTION

Chemosensory information is crucial for the survival of humans and other animals. For example, a large part of animal behavior, including control of emotional states, food intake, and social interactions, relies on the capacity to perceive odor information and to retrieve its potential meaning based on previous experiences [1, 2]. Olfactory perception starts when odorant molecules, traveling through orthonasal or retronasal pathways, reach olfactory receptors on sensory neurons located in the olfactory epithelium [3]. These neurons project to the olfactory bulb that in turn transmits the signal to other brain regions, including the anterior piriform cortex (aPC) [4, 5], which plays a key role in olfactory processing and memory [6–8]. However, the specific cellular mechanisms governing odor information storage and retrieval in the aPC are still unclear.

Cannabinoid type-1 (CB1) receptors together with their endogenous ligands (endocannabinoids) form the core of the so-called endocannabinoid system (ECS) in the brain [9], which is an important modulator of many functions, including learning and memory [10, 11]. Activation of presynaptic CB1 receptors is well-known to physiologically control the release of several neurotransmitters in many brain regions [12, 13]. CB1 receptors are present in different olfactory structures [14], where they can modulate olfactory processes [15–19]. However, little is known about the specific impact of CB1 receptor signaling in olfactory brain structures on odor-dependent memory functions.

Considering that the aPC is an important region for olfactory memory [6–8, 20–22], we hypothesized that CB1 receptors in the aPC (aPC-CB1) could modulate odor-related memory processes. Our data show that aPC-CB1 receptors are specifically required for the expression of appetitive, but not aversive, olfactory memory, and they are involved in the direct control of the associated modulation of local inhibitory circuits. Altogether, these results indicate that the physiological activation of CB1 receptors in the aPC exerts a fine-tuned regulation of olfactory circuits and functionally discriminates the retrieval of positively and negatively motivated olfactory memories.

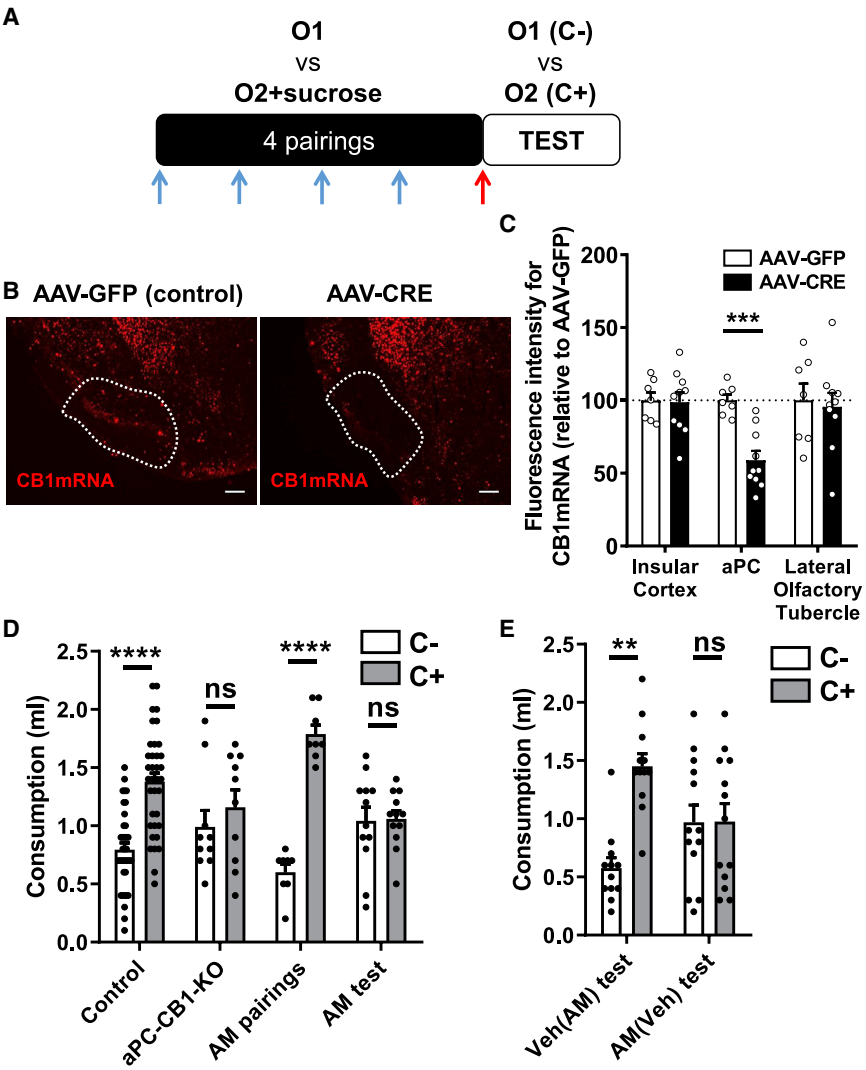

Figure 1. CB1 Receptors in the aPC Are Necessary for Retrieval of Odor Preference

(A) Schematic protocol used for conditioned odor preference (COP). During conditioning, the two odor-scented solutions (O1 and O2) are associated to the absence or presence of sucrose, becoming neutral (C−) or conditioned (C+) stimuli, respectively. Blue arrows, aPC infusions before pairings; red arrow, aPC infusion before test for pharmacological experiments.

(B) Representative images of fluorescent *in situ* hybridization against CB1 mRNA (red), showing the virally induced deletion of CB1 receptors in the aPC of *CB1*-Flox mice locally injected with adeno-associated virus (AAV)-GFP or AAV-CRE. Scale bars, 200 μm.

(C) Quantification of fluorescence intensity of CB1 mRNA in the insular cortex, the aPC, and the lateral olfactory tubercle from sections where maximal deletion of CB1 expression was observed in aPC-*CB1*-KO and from equally located sections in control mice (n = 7–10).

(D) Consumption of C+ and C− odor-scented solutions in control mice (control; n = 36), mice carrying deletion of aPC-CB1 receptors (aPC-*CB1*-KO; n = 10), and mice receiving aPC infusions of the CB1 receptor antagonist AM251 (4 μg/0.5 μL per side) before each odor-sucrose pairing (AM pairings; n = 8) or before the COP retrieval test (AM test; n = 12).

(E) Consumption of C+ and C− solutions during a second COP retrieval test performed after re-training (STAR Methods). Mice previously infused with AM were infused with vehicle before the second test ("Veh(AM) test"; n = 12), and those previously infused with vehicle were now infused with AM ("AM(Veh) test"; n = 13).

**p < 0.01; ***p < 0.001; ****p < 0.0001; ns, not significant. For statistical details, see Tables S1, S2, and S3. For supplemental information, see Figures S1 and S2.

RESULTS

CB1 Receptors in the aPC Are Necessary for the Retrieval of Conditioned Odor Preference

To investigate the potential impact of CB1 receptor signaling in odor-related memory, we set up a behavioral protocol to assess conditioned odor preference (COP) in mice (STAR Methods; Figures 1A, S1A, and S1B) [23, 24]. Using this protocol, mice displayed a reliable preference for the odor-scented solution previously associated to sucrose (C+) as compared to the other one (C−), revealing the formation of COP (Figure S1C), regardless of the odor used as C+ (Figures S1D and S1E).

We next investigated the role of CB1 receptors in the aPC (aPC-CB1) during COP. Specific deletion of the *CB1* gene in the aPC (aPC-*CB1*-KO; STAR Methods; Figures 1B, 1C, and S1F–S1I) [25–27] abolished the preference for the C+ solution during test (Figure 1D), without altering sucrose preference upon training (Figure S1J) or total liquid intake (Figure S1K) and independently from the anatomical extension of the CB1 deletion (Figure S1L). These results indicate that COP requires aPC-CB1 receptors. To determine the specific role of CB1 receptor signaling in the different phases of the COP protocol, we acutely injected the CB1 receptor antagonist AM251 into the aPC (4 μg/0.5 μL per side; Figures S2A–S2E) prior to each odor-sucrose pairing or before the retrieval test (Figure 1A). Neither consumption during training nor COP performance were affected by aPC-CB1 blockade before each pairing (AM pairings; Figures 1D, S1J, S1K, and S2F). Conversely, AM251 acutely injected into the aPC prior to the retrieval test abolished COP, without altering total liquid consumption (AM test; Figures 1D, S1J, S1K, and S2F). Acute blockade of aPC-CB1 receptors might permanently impair COP retrieval. On the other hand, longer training might render COP retrieval independent of aPC-CB1 receptors. To simultaneously test for these possibilities, animals previously treated with AM251 or vehicle received 4 additional odor-sucrose pairings (STAR Methods) and were injected with vehicle ("Veh(AM) test") or AM251 ("AM(Veh) test") before the second retrieval test, respectively. In these conditions, vehicle-treated mice displayed clear COP, whereas AM251 blocked this behavior (Figures 1E and S2G). aPC-CB1 receptors might control expression of preference independently of previous learning.

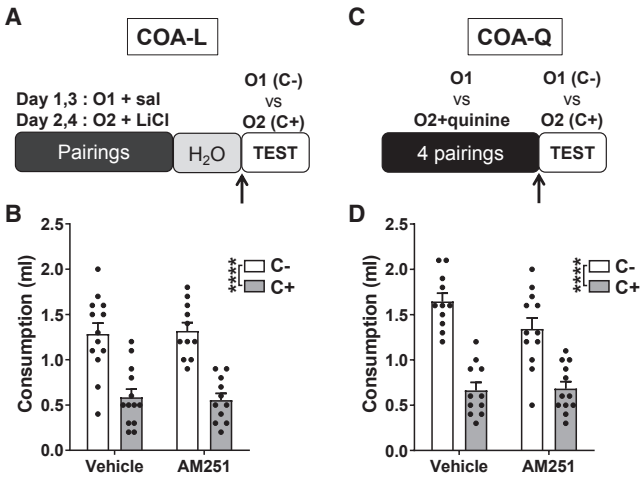

Figure 2. CB1 Receptors in the aPC Are Not Involved in the Retrieval of Odor Aversion

(A) Schematic representation of the protocol used for LiCl-induced conditioned odor aversion (COA-L).

(B) Consumption of the odor-scented solutions (C+ and C−) during test of COA-L in mice receiving aPC infusions of the CB1 receptor antagonist AM251 (4 μg/0.5 μL per side; n = 11) or vehicle (n = 13).

(C) Schematic representation of the protocol used for quinine-induced conditioned odor aversion (COA-Q).

(D) Consumption of the odor-scented solution during test of COA-Q in mice receiving aPC infusions of AM251 (n = 12) or vehicle (n = 11).

C+, odor-scented solutions previously paired with LiCl injections (B) or quinine (D); C−, odor-scented solutions paired with saline injections (B) or water (D). Black arrows, time of intra-aPC infusions. ****$p < 0.0001$ general solution effect. For statistical details, see Tables S1, S2, and S3. For supplemental information, see Figures S2 and S3.

However, aPC-CB1 blockade did not impair innate sucrose preference (Figures S3A–S3C).

Altogether, these results indicate that endogenous activation of aPC-CB1 is specifically required during retrieval of COP, without affecting innate responses to attractive stimuli.

CB1 Receptors in the aPC Are Not Involved in the Retrieval of Conditioned Odor Aversion

We next asked whether aPC-CB1 receptors are also involved in the retrieval of conditioned odor aversion (COA) induced by lithium chloride (LiCl) injections (Figure 2A; COA-lithium [COA-L]) [25, 28–30]. Notably, AM251 acutely injected into the aPC did not impair COA-L expression (Figures 2A, 2B, S2A–S2F, and S3D), suggesting that aPC-CB1 receptors are dispensable for the retrieval of negatively motivated olfactory memory. However, the differential effects of CB1 receptor blockade between COP and COA-L could be due to the different types of associations involved (sensory-sensory versus sensory-gastric). Using a sensory-sensory COA protocol, where sucrose was substituted by the aversive taste quinine (COA-Q; Figures 2C and S3E) [31, 32], mice treated with vehicle or the CB1 receptor antagonist before the retrieval test displayed the same avoidance toward the conditioned odor (Figures 2D, S2F, and S3F).

Altogether, these data indicate that aPC-CB1 receptor signaling is necessary for the retrieval of COP, but not of COA, suggesting that expression of acquired odor choices rely on different mechanisms depending on the valence of the unconditioned stimulus.

CB1 Receptors Are Highly Expressed in GABAergic Interneurons in the aPC

As previously reported [14, 33], fluorescent immunohistochemistry revealed that CB1 receptor protein is highly expressed in layer II of the aPC (Figure 3A), where the aPC principal neurons are mainly localized [34, 35]. To detail the cellular distribution of CB1 receptors, we analyzed aPC tissues from conditional mutant mice carrying exclusive expression of the protein in identified specific cell types (rescue mice) [33, 36, 37]. A similar pattern of CB1 receptor immunoreactivity was observed across aPC tissues from wild-type (WT) mice and global CB1-rescue mice (Figure 3A) [33, 37] but also from mice with specific re-expression in GABAergic neurons (GABA-CB1 rescue; Figure 3A) [33, 36]. In contrast, the immunoreactivity was extremely low in mice re-expressing the receptor only in cortical glutamatergic neurons (Glu-CB1 rescue; Figure 3A) [37] and, as expected, was undetectable in mice where CB1 receptor expression is absent (CB1 stop; Figure 3A) [33, 36, 37]. To better characterize the expression of CB1 receptors at the synaptic level, we next used immunogold electron microscopy (Figure 3B). As expected, CB1 receptor immunogold particles were specifically present in different amounts at many cellular locations (Figures 3B and S4). Among CB1 receptor particles located at terminals (1,856 over 3,409 total counted in WT; Figures 3B and S4), approximately 88% and 12% were at symmetric (presumably inhibitory) and asymmetric synapses (presumably excitatory), respectively (Figures 3B and 3C). Moreover, whereas only 23% of excitatory terminals were labeled with CB1 receptor immunogold particles, this percentage was as high as 87% in inhibitory ones (Figures 3B and 3D). As expected, only background staining was detected in sections from *CB1*-KO mice (18 particles at terminals; Figures 3B, 3D, and S4).

To identify the specific topographical distribution of CB1-expressing cells within the aPC, we used double fluorescent *in situ* hybridization (D-FISH) to label the mRNAs of CB1 receptor and of glutamic acid decarboxylase 65 kDa (GAD), a marker of GABAergic neurons (Figure 4A). Consistent with previous studies [38], the majority of GAD-expressing cells were observed in deep layer III (Figures 4A and 4B). CB1 mRNA was also highly expressed in layer III, with scattered positive cells in layer I (Figures 4A and 4C). Accordingly, counting of positive cells revealed that a high proportion of GAD+ neurons contained also CB1 mRNA (63%; Figures 4A and 4D), following the distribution of GAD across layers (Figures 4A, 4B, and 4E). Similarly to other cortical regions, such as the hippocampus [39], CB1 mRNA was expressed at very different levels across CB1-positive aPC cells. Whereas a majority of cells expressed low-to-moderate amounts of the transcript, scattered cells contained very high levels of CB1 mRNA, especially in layers II and III (Figure 4A). Interestingly, virtually 100% of these high CB1-expressing neurons co-expressed GAD mRNA (Figure 4F). Conversely, low CB1-expressing neurons were virtually all identified as GAD-positive in layer I, but this proportion was reduced in layers II and III (Figure 4F).

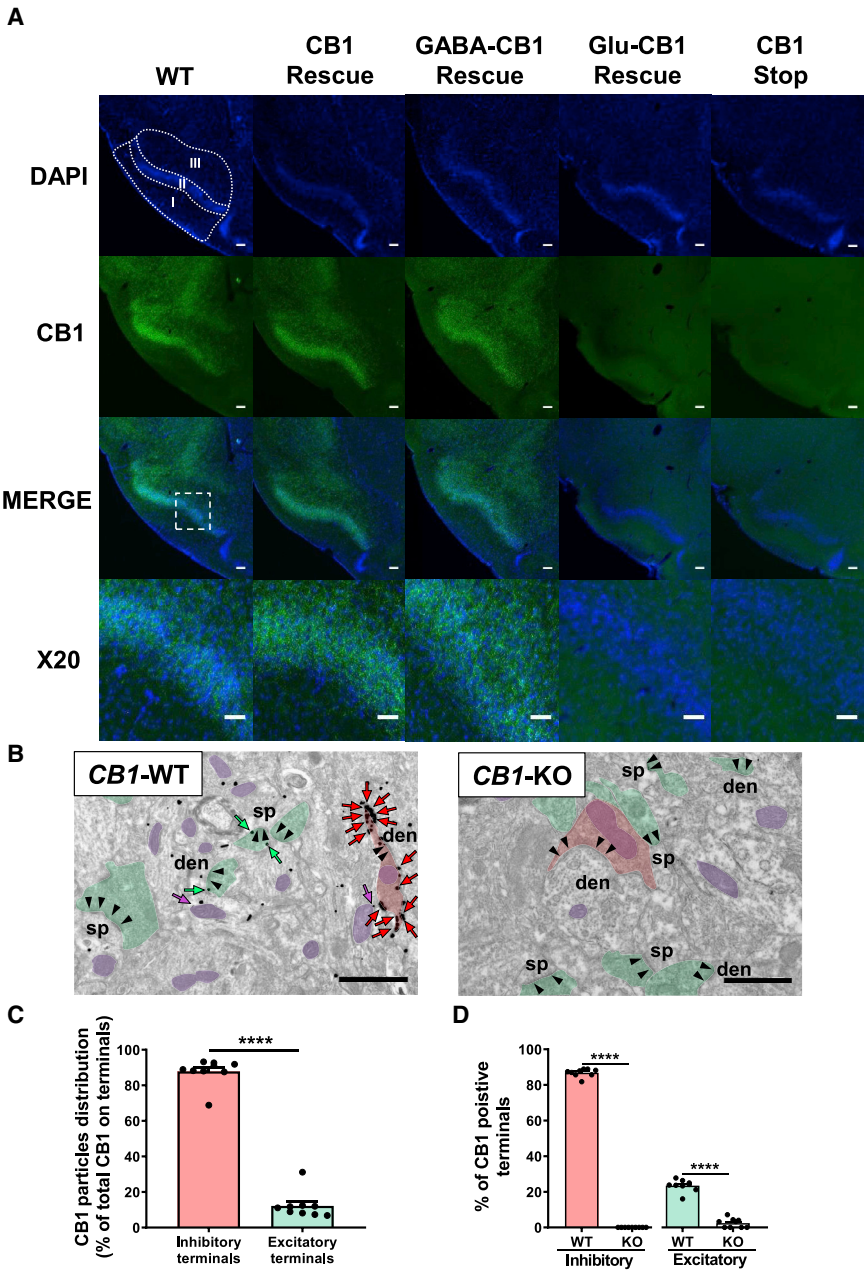

Figure 3. CB1 Receptors Are Highly Expressed in GABAergic Interneurons in the aPC

(A) Representative coronal brain sections showing immunostaining of CB1 receptors in the aPC of wild-type (WT), CB1 rescue, GABA-CB1 rescue, Glu-CB1 rescue, and CB1 stop mice. Dotted lines delimitate the different cortical layers (I, II, and III). Scale bars, 100 μm.

(B) Electron microscopy micrographs of immunogold staining for CB1 receptors in the aPC of CB1 wild-type (*CB1*-WT) and knockout mice (*CB1*-KO). Black arrowheads, synapses; den, dendrites; sp, spines; red areas, presumably inhibitory terminals and preterminals; green areas, presumably excitatory terminals; purple areas, mitochondria; red arrows, CB1 receptors on inhibitory terminals and pre-terminals; green arrows, CB1 receptors on excitatory terminals; purple arrows, CB1 receptors on mitochondria. Scale bars, 1 μm.

(C) Proportion of CB1 receptor immunoparticles on inhibitory and excitatory terminals over total CB1 labeling on terminals (100%).

(D) Percentage of CB1-receptor-labeled inhibitory and excitatory terminals in *CB1*-WT and *CB1*-KO. ****$p < 0.0001$. For statistical details, see Tables S1, S2, and S3. For supplemental information, see Figure S4.

Altogether, these data indicate that the large majority of aPC-CB1 receptor proteins is expressed in terminals of local GABAergic neurons, with layer-specific topographical distribution.

CB1 Receptors Control Inhibitory Transmission in the aPC

To start addressing the so-far-unexplored cannabinoid-dependent control of inhibitory transmission in the aPC, we first determined by *ex vivo* patch-clamp electrophysiological recordings the impact of CB1 receptor activation on GABAergic neurotransmission impinging onto specific populations of principal cells of the aPC (semilunar-like neurons [SL] and pyramidal-like neurons [PNs]; Figures S5A and S5B; STAR Methods).

These cells receive many inputs from the olfactory bulb and other brain regions, project to other olfactory cortical areas [35, 40, 41], and are extensively innervated by local inhibitory interneurons [38, 42, 43]. Thus, we reasoned that selective modulation of GABAergic inputs onto SL cells and/or PNs might represent a way through which CB1 receptors rapidly regulate principal cell activity and consequently odor processing. To address this possibility, we recorded miniature inhibitory post-synaptic currents (mIPSCs) representing the global inhibitory inputs of principal cells. These events occur at a frequency of 2.06 ± 0.23 Hz and an amplitude of 76.29 ± 4.41 pA (Vehicle; Figures 5A–5C) in SL cells and at a frequency of 2.50 ± 0.39 Hz and an amplitude of 64.06 ± 4.27 pA in PNs of naive animals (Vehicle; Figures 5D–5F). Similarly to what was observed in the hippocampus [44], the application of the CB1 receptor agonist WIN 55,212-2 (WIN; 5 μM) significantly reduced the frequency of mIPSCs in SL cells, with only a slight impact, if any, on their amplitude (Figures 5A–5C), suggesting a presynaptic inhibitory effect. This decrease was fully reversed by the application of the CB1 receptor antagonist AM251 (WIN+AM251; 4 μM; Figures 5A–5C). Conversely and surprisingly, no such effects were observed in PNs (Figures 5D–5F), indicating a cell-type-specific impact of CB1-receptor-dependent control of inhibitory currents in naive animals.

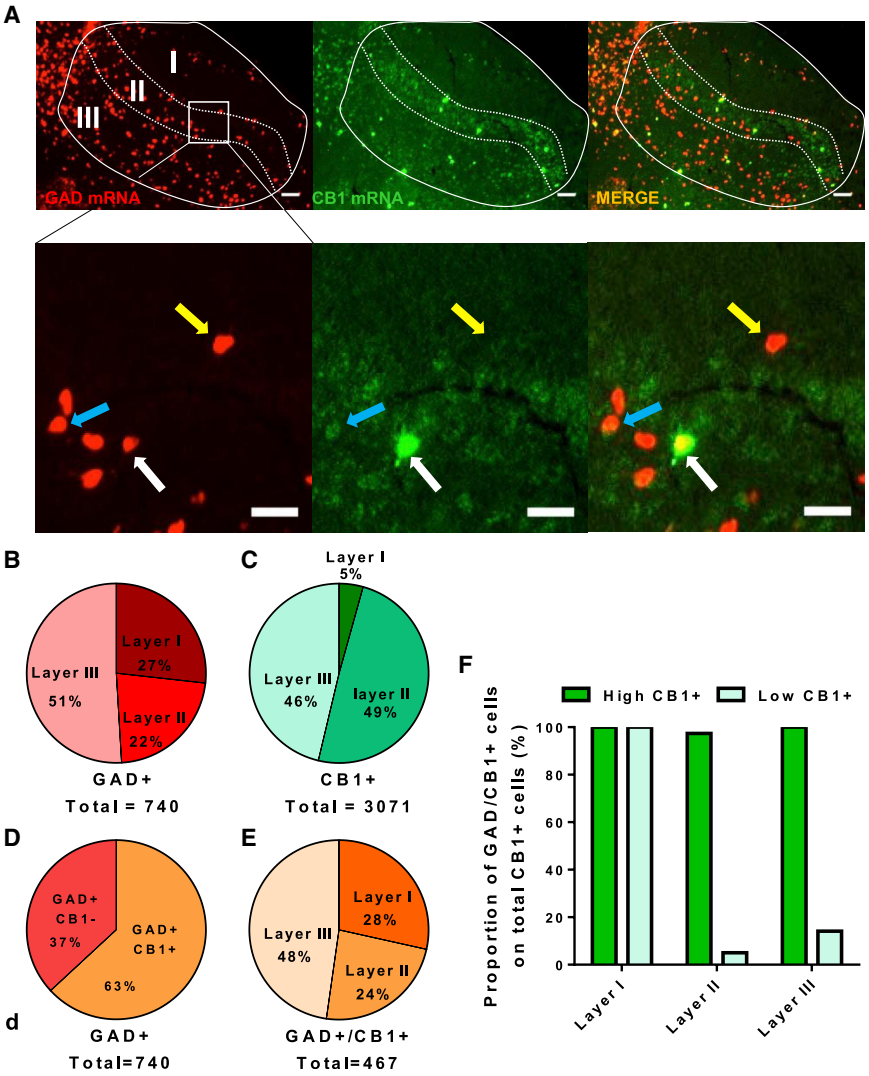

Figure 4. Topographic Distribution of CB1-Receptor-Positive GABAergic Interneurons in the aPC

(A) Representative images showing double fluorescent *in situ* hybridization (D-FISH) of GAD 65 kDa mRNA (GAD, red) and CB1 mRNA (green) in the aPC. Lower panels, higher magnifications of the boxed in the top panels; yellow arrows, GAD-positive cells that do not express CB1; blue arrows, GAD-positive cells containing low levels of CB1 mRNA; white arrows, GAD-positive cells containing high levels of CB1 mRNA. Lines in top panels delimitate the different cortical layers (I, II, and III). Scale bars, 100 μm (top) and 50 μm (bottom).

(B–E) Pie charts representing percentage distribution of (B) cells expressing GAD mRNA in different layers, (C) cells expressing CB1 mRNA in different layers, (D) GAD-positive cells expressing or not CB1 mRNA, and (E) cells expressing both GAD and CB1 mRNAs in different layers. Total numbers of counted cells are below each chart (n = 118 sections from 4 animals).

(F) Percentages of GAD mRNA expression in total high- (green) and low-CB1-expressing cells (light green) in the different layers of the aPC.

In summary, CB1 receptors are highly expressed in GABAergic interneurons of the aPC, and their activation results in the modulation of inhibitory inputs onto SL principal neurons.

COP Retrieval Reduces mIPSCs in the aPC via Presynaptic CB1 Receptors

We next hypothesized that retrieval of COP might be associated with aPC-CB1 receptor-dependent modulation of principal cells' mIPSCs. A significant reduction of mIPSC frequency (~26%) was found in SL cells from mice sacrificed during COP retrieval, as compared to a control group exposed to the same number of only water-drinking sessions (Water; Figures 6A and 6B). SL cells from mice receiving the same number of "training" sessions but without the presence of sucrose (Sucrose free) or odor (Odor free) did not display any reduction of mIPSC frequency (Figure 6B). Considering that aPC-CB1 receptors regulate COP, but not COA, retrieval (Figures 1 and 2), we next evaluated the effect of COA-Q retrieval, and we found that this condition did not affect mIPSC frequency (Figure 6B). Notably, no differences in amplitudes were observed across the groups (Figure S6A). Altogether, these results indicate that COP retrieval, but not exposure to odor or sucrose alone or COA retrieval, is associated with a specific reduction of presynaptic inhibitory transmission onto SL neurons in the aPC.

As local blockade, the systemic injection of the CB1 receptor antagonist rimonabant (Rim) (1 mg/kg) impaired COP retrieval (Figures 6C and S6B), independently of total liquid consumption (Figures S6C–S6F). As expected, systemic injection of vehicle before COP retrieval did not alter the associated reduction of mIPSCs frequency in SL cells (Figures 6D and 6E; $p > 0.8$, as compared to Figure 6B). Conversely, systemic administration of Rim abolished this decrease up to levels undistinguishable from control mice (Figures 6D and 6E; $p > 0.8$, as compared to Figure 6B), with no effect on amplitude (Figure S6G). Notably, mIPSC frequencies, but not amplitudes, of individual animals were inversely correlated with the COP retrieval performance (Figure 6F; data not shown), suggesting that the level of presynaptic inhibition of SL cells is linked to the behavioral retrieval of COP.

Next, we examined the impact of COP retrieval on mIPSCs of PNs. Similarly to SL neurons, the frequency of mIPSCs was reduced (~33%) in PNs of animals undergoing COP retrieval, as compared to water control mice (Figures 6G and 6H) with no change in amplitude (Figure S6H). A slight non-significant increase of mIPSCs amplitude was observed in PNs from mice receiving systemic injection of Rim prior to COP retrieval (Figure S6H). However, this treatment was not able to reverse the COP-retrieval-associated reduction of mIPSCs frequency in PNs (Figures 6G and 6H). No correlations between COP retrieval and the levels of mIPSC frequencies or amplitudes of

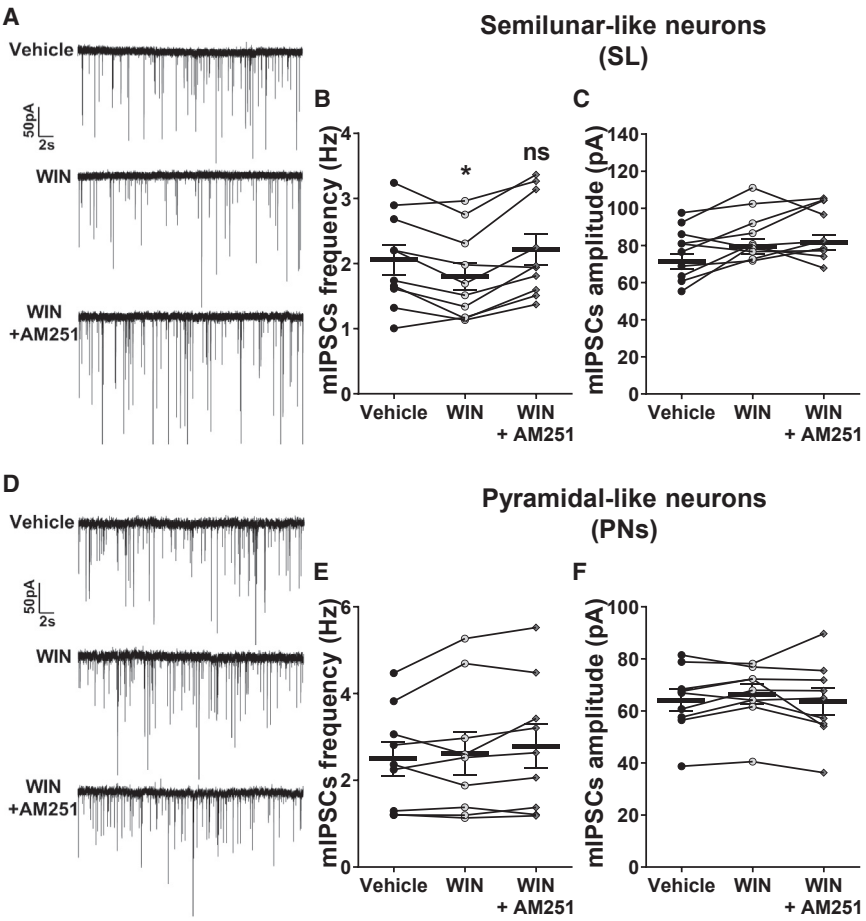

Figure 5. CB1 Receptors Control Inhibitory Transmission in SL Cells of the aPC

(A) Representative traces of miniature inhibitory postsynaptic currents (mIPSCs) recorded in aPC semilunar-like neurons (SL) under different sequential treatments: Vehicle; WIN, CB1 receptor agonist WIN55,212-2 (5 μM); WIN + AM251, WIN together with the CB1 receptor antagonist AM251 (4 μM).

(B and C) Quantifications of mIPSCs frequency (B) and amplitude (C) recorded in SL cells under Vehicle, WIN, and WIN+AM251 treatments (n = 10 cells from 4 mice).

(D) Representative traces of mIPSCs recorded in aPC pyramidal-like neurons (PNs) under the same sequential treatments as in (A)–(C).

(E and F) Quantifications of mIPSCs frequency (E) and amplitude (F) recorded in PNs under the different treatments (n = 9 cells from 5 mice). *p < 0.05 (versus vehicle).

For statistical details, see Table S1. For supplemental information, see Figure S5.

PNs in individual mice were observed (Figure 6I; data not shown).

Altogether, these results indicate that COP retrieval is associated to a reduction of inhibitory inputs on both SL cells and PNs. However, presynaptic CB1 receptors appear to regulate inhibitory transmission in the aPC in a cell-type-specific manner, thereby providing an unforeseen fine-tuned modulation of olfactory memory circuits, likely contributing to appropriate behavioral responses.

Acute Blockade of CB1 Receptors Affects COP Retrieval through GABAergic Neurons

We then addressed the potential involvement of CB1 receptors expressed in inhibitory neurons (GABAergic CB1) in COP retrieval. Surprisingly, mice lacking *CB1* gene expression from GABAergic neurons (GABA-*CB1*-KO) [27, 45] did not display any alteration of COP retrieval as compared to control wild-type littermates (GABA-*CB1*-WT; Figure S6I). This negative result might suggest that CB1 receptors in GABAergic neurons are not necessary for acute COP retrieval. However, GABA-*CB1*-KO mice carry a deletion of CB1 receptors in all GABAergic cells of the whole forebrain, starting from early developmental stages [27, 46]. Such diffuse and long-lasting absence of CB1 receptor signaling might induce opposing effects in different brain regions and/or stimulate developmental compensatory phenomena, whose general mechanisms recently started to be elucidated [47, 48]. If occurring in GABA-*CB1*-KO mice, these mechanisms might mask the specific acute role of CB1 receptors signaling in GABAergic neurons in COP retrieval during adulthood. Considering this possibility, we adopted an alternative strategy to investigate the specific role of CB1 receptors in GABAergic neurons, by testing whether the blockade of COP retrieval by the acute administration of Rim was still effective in GABA-*CB1*-KO mice. A systemic acute injection of the drug blocked COP retrieval in GABA-*CB1*-WT, but it failed to impair this behavior in GABA-*CB1*-KO mice (Figures 6J, 6K, and S6J–S6L), indicating that CB1 receptors in GABAergic neurons are required for the COP-retrieval-disrupting effect of the acute pharmacological blockade of CB1 receptor signaling.

DISCUSSION

In this study, we functionally characterized the presence and the role of CB1 receptors in the aPC. We found that these receptors are specifically involved in the retrieval of appetitive, but not aversive, olfactory memory and in the associated modulation of inhibitory transmission onto specific aPC principal cells. Moreover, our data show that the retrieval impairment of appetitive olfactory memory induced by CB1 antagonism requires CB1 receptors expressed in inhibitory neurons.

aPC-CB1 Receptors Are Necessary for the Retrieval of Appetitive, but Not Aversive, Olfactory Memory

In other brain structures, CB1 receptors have been reported to play crucial roles in different phases of learning and memory processes [10, 11]. Our data reveal that the endogenous activation of aPC-CB1 receptors is necessary for COP retrieval, but it is dispensable for its acquisition, thereby enlarging the spectrum of CB1 receptor involvement in different phases of learning and

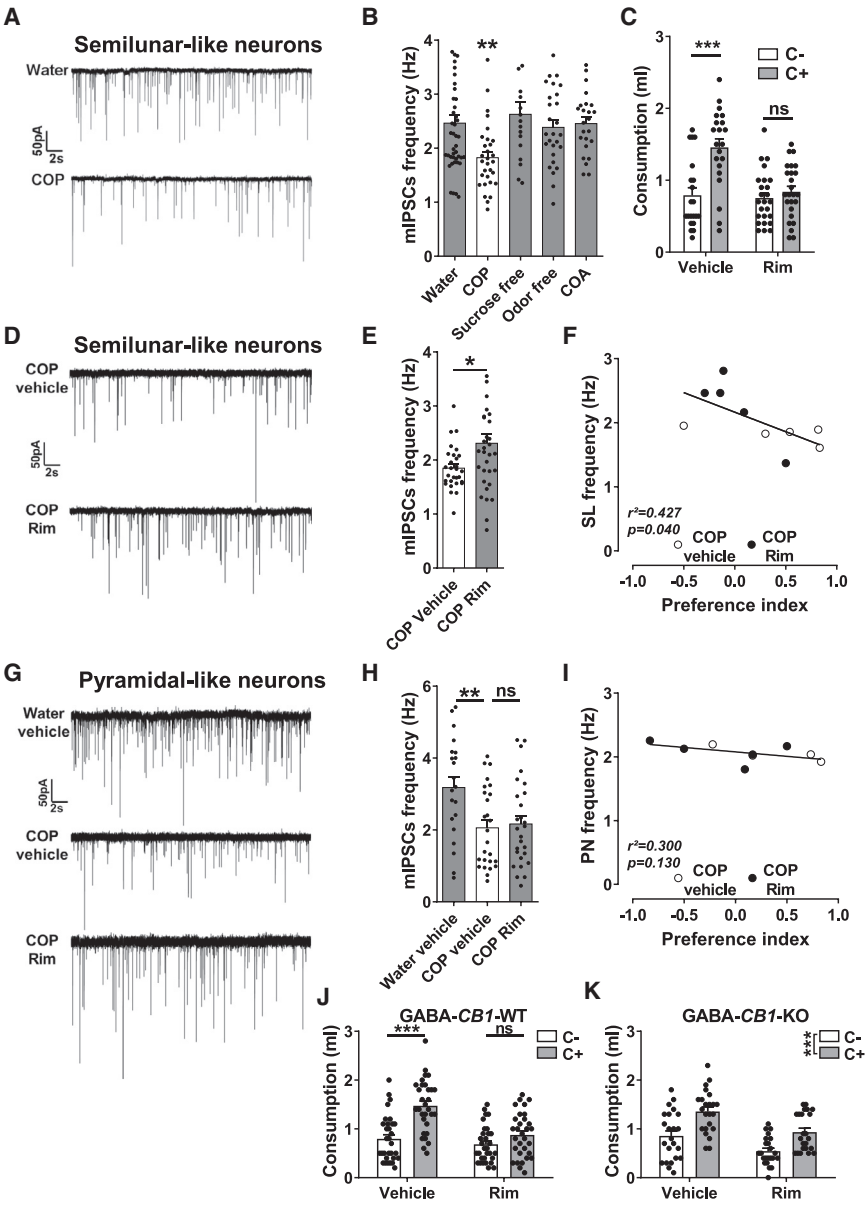

Figure 6. Involvement of GABAergic Transmission in the CB1-Receptor-Dependent Control of COP Retrieval

(A) Representative traces of mIPSCs recorded in SL neurons in the aPC, from mice sacrificed during control water consumption (Water) or COP retrieval test (COP).

(B) Quantifications of mIPSCs frequency in SL neurons of mice sacrificed during water consumption (Water; n = 44 cells from 10 animals), COP retrieval test (COP; n = 30 cells from 8 animals), exposure to odor-scented solutions without sucrose (Sucrose free; n = 17 cells from 4 animals), exposure to sucrose solution without odors (Odor free; n = 27 cells from 4 animals), or COA retrieval test (COA; n = 24 cells from 4 animals).

(C) Consumption of C+ and C− during COP retrieval test after administration of vehicle or the CB1 receptor antagonist rimonabant (intraperitoneal [i.p.], Rim, 1 mg/kg).

(D–F) Effect of i.p. injections of vehicle or Rim on mIPSCs of SL cells from mice sacrificed during COP retrieval test.

(D) Representative traces.

(E) Quantification of mIPSCs frequency (COP Vehicle, n = 30 cells from 5 animals; COP Rim, n = 32 cells from 5 animals).

(F) Correlation between the average of mIPSC frequencies in SL neurons of individual animals and their COP retrieval performances expressed as preference index (COP Vehicle, n = 5; COP Rim, n = 5).

(G–I) Effect of i.p. injections of vehicle or Rim on mIPSCs of PNs in mice sacrificed during water consumption (Water Vehicle) or COP retrieval test (COP Vehicle and COP Rim).

(G) Representative traces.

(H) Quantification of mIPSCs frequency (Water Vehicle, n = 21 from 3 animals; COP Vehicle, n = 26 from 4 animals; COP Rim, n = 27 from 5 animals).

(I) Correlation between the average of mIPSC frequencies in PNs from individual animals and their COP retrieval performances, expressed as preference index (COP Vehicle, n = 4; COP Rim, n = 5).

(J and K) Consumption of the C+ and C− odor-scented solutions in (J) GABA-*CB1*-WT (n = 31) and in (K) GABA-*CB1*-KO mice (n = 23) receiving i.p. injections of either vehicle or Rim before a COP test (STAR Methods).

*p < 0.05; **p < 0.01; ***p < 0.001. For statistical details, see Tables S1 and S3. For supplemental information, see Figures S5 and S6.

memory. Interestingly, it was recently found that a small enhancement of hippocampal GABAergic inhibition blocked cell firing and memory retrieval but left memory encoding intact [49]. This nicely parallels our results showing that a small but CB1-receptor- and cell-type-dependent reduction in GABAergic inhibition in the aPC is associated with effective COP memory retrieval. We here propose that CB1 receptors on GABAergic axon terminals might be essential to reduce inhibition onto SL cells, thereby permitting cell firing in the ensemble population to retrieve the COP memory trace. In this context, it is interesting to note that COP retrieval is also associated with a similar reduction of inhibitory drive onto PNs, but in a CB1-receptor-independent manner. This suggests that cell-type-specific mechanisms are involved in the coordinated regulation of the activity of distinct aPC principal neurons during retrieval of olfactory memory.

Our data show that the retrieval of aversive olfactory memory is independent of aPC-CB1 receptor signaling. These intriguing results might be explained by two possibilities: either COA depends on aPC but it does not involve CB1 receptor signaling or COA does not depend on aPC. There is currently no clear answer to this question, but some pieces of evidence seem to indicate a certain level of specialization of the aPC for positively motivated olfactory memory. Optogenetic or chemogenetic manipulations of selected neurons in the PC can modulate both aversive and appetitive behavioral responses [50, 51]. Despite the fact that specific aPC activity was observed during COA retrieval [52],

olfactory cues associated with sucrose activate more aPC neurons than odors associated with quinine [53] and aPC lesions impair appetitive, but not aversive, odor-related memory [21]. In addition, CB1 receptor signaling can mediate aversive olfactory memory in other brain regions. For instance, Laviolette and Grace [54] showed that CB1 receptors in the medial prefrontal cortex are required for odor-dependent fear conditioning, and we recently demonstrated that deletion of the *CB1* gene specifically in medial habenular neurons selectively abolishes COA, but not COP [30]. Moreover, it has been shown that the basolateral nucleus of the amygdala (BLA), which is essential for COA [31, 55], is more strongly connected with the posterior PC (pPC) than with the aPC [56], and BLA-pPC interactions are important for aversive odor conditioning [57]. Conversely, the aPC is more densely connected than the pPC to the olfactory tubercle, which, by receiving intense dopaminergic inputs, might be specifically involved in the processing of reward-related information [58]. Altogether, this suggests a potential double dissociation in the roles of aPC and pPC in COP and COA, with the aPC being somehow specialized in processing positive acquired values of odors and the pPC more involved in aversive odor memory.

CB1 Receptors Are Highly Expressed in aPC GABAergic Interneurons and Regulate Local Inhibitory Neurotransmission

Our immunohistochemical, D-FISH and electron microscopy data show that CB1 receptors are found in a high proportion of GABAergic neurons located in the three layers of the aPC and that they are strongly expressed at inhibitory synaptic terminals. Moreover, pharmacological activation of aPC-CB1 receptors decreases miniature inhibitory currents frequency specifically in SL cells. Similarly to the hippocampus [39], cells expressing high levels of CB1 mRNA are exclusively GABAergic interneurons. Recent evidence points to the presence of long-range inhibitory neurons as a novel neuroanatomical and functional feature in cortical areas [59]. These putative long-range inputs to the aPC might contain CB1 receptors, but our viral manipulations exclude their participation in the CB1-receptor-dependent retrieval of COP. Interestingly, depending on the layer, a portion of low CB1-expressing cells do not co-express GAD mRNA and are presumably glutamatergic neurons. Indeed, CB1 receptor protein is abundantly present in the main olfactory bulb at terminals of glutamatergic centrifugal fibers coming from principal neurons of the anterior olfactory nucleus and aPC [18]. Importantly, as these "glutamatergic" CB1 receptors play a key role in the control of olfactory perception and food intake [18], we cannot fully exclude that alterations in olfactory perception might participate in the phenotype of aPC-*CB1*-KO mice. However, intra-aPC pharmacological manipulations indicate that local CB1 receptor signaling is necessary for COP retrieval, but it is dispensable for expression of COA. Therefore, any putative impairment of olfactory perception induced by deletion of the *CB1* gene in projecting glutamatergic neurons of the aPC is unlikely to be responsible for the phenotype of aPC-*CB1*-KO mice. Nevertheless, our electron microscopy immunogold results indicate that a small proportion of CB1 receptors are specifically present at glutamatergic terminals within the aPC. Moreover, a consistent portion of CB1 receptors appears to be located outside of terminals. Future studies will investigate the origin and the potential roles of these aPC subpopulations of CB1 receptors, which might still have functional significance.

COP Retrieval Is Associated with CB1-Receptor-Dependent Modulation of Inhibitory Transmission on Specific aPC Principal Cells

An approximate 30% decrease of mIPSCs frequency recorded in both aPC SL cells and PNs was observed in slices from mice undergoing COP retrieval. In PNs, CB1 receptor antagonism did not affect COP-dependent frequency decrease. Conversely, the same treatment fully reversed mIPSCs frequency in SL cells up to the same levels of mice exposed to water alone, odor alone, sucrose alone, or COA. Together with the fact that mIPSCs amplitude was not affected and that frequency values were inversely correlated with behavioral performance, these results indicate that COP retrieval is likely associated with presynaptic reduction of inhibitory transmission onto aPC SL cells. This idea is reinforced by the fact that the COP retrieval impairment under pharmacological CB1 receptor blockade is absent in mice lacking CB1 receptors from forebrain GABAergic neurons.

Hence, these results suggest that aPC-CB1 receptors control the behavioral responses induced by appetitive olfactory memory by regulating cell-type-specific inhibitory transmission. More generally, they imply a dissociation between the roles of SL cells and PNs in the processing of olfactory information that will be very interesting to study in deeper details.

Interestingly, inhibitory circuits within the aPC have been shown to be strongly recruited in olfactory-dependent processes [43, 60–62]. For instance, *in vivo* odor exposure widely activates GABAergic interneurons in the aPC [43], potentially participating in the processing of odors and their meaning [63]. In this context, the spatially restricted functions of CB1 receptors (i.e., on SL cells, but not on PNs) suggest that CB1-receptor-dependent processes selectively tune the excitability of specific aPC principal neurons during COP retrieval. These processes would, in turn, refine the response to positively conditioned odor stimulations, eventually allowing the precise "funneling" of behavior toward preference responses.

In conclusion, this study provides a first characterization of the functional role of CB1 receptor signaling in aPC circuitry and related behaviors, thereby contributing to a better understanding of how the aPC participates in specific memory functions.

STAR★METHODS

Detailed methods are provided in the online version of this paper and include the following:

- KEY RESOURCES TABLE
- LEAD CONTACT AND MATERIALS AVAILABILITY
- EXPERIMENTAL MODEL AND SUBJECT DETAILS
- METHOD DETAILS
  - Behavioral procedures
  - Surgery
  - Drugs
  - Immunohistochemistry
  - Immunocytochemistry for electron microscopy
  - Fluorescent *in situ* hybridization
  - Electrophysiology

SUPPLEMENTAL INFORMATION

Supplemental Information can be found online at https://doi.org/10.1016/j.cub.2019.06.041.

ACKNOWLEDGMENTS

We thank all the personal of the Animal Facility of the NeuroCentre Magendie for mouse care and genotyping. We also thank Gabriel Lepousez, Antoine Nissant, Pierre-Marie Lledo, and all the members of Marsicano's lab for useful discussions. This work was supported by INSERM (to G.M.), INRA (to G.F.), Fondation pour la Recherche Médicale (DRM20101220445 to G.M. and FDT20170436845 to G.T.), French State/Agence Nationale de la Recherche (LABEX BRAIN ANR-10-LABX-43 to G.M., G.F., and A.B.-G.; ANR-10-IDEX-03-02 to A.B.-G.; NeuroNutriSens ANR-13-BSV4-0006-02 to G.M.; Orups ANR-16-CE37-0010 to G.M. and G.F.; CaCoVi ANR-18-CE16-0001 to G.M.; and MitObesity ANR-18-CE14-0029 to G.M.), EU–FP7 (PAINCAGE, HEALTH-603191 to G.M.; FP7-PEOPLE-2013-IEF-623638 to A.B.-G.), European Research Council (Endofood, ERC–2010–StG–260515, CannaPreg, ERC-2014-PoC-640923, and MiCaBra, ERC-2017-AdG-786467 to G.M.), Human Frontiers Science Program (to G.M.), Region Aquitaine (to G.M.), Fyssen Foundation (to E.S.-G.), MINECO/FEDER, UE (SAF2015-65034-R to P.G.), The Basque Government (BCG IT764-13 to P.G.), Red de Trastornos Adictivos, Instituto de Salud Carlos III (ISC-III), and European Regional Development Funds-European Union (ERDF-EU) (RD16/0017/0012 to P.G.).

AUTHOR CONTRIBUTIONS

G.T., G.F., and G.M. designed research; G.T., M.V., S.A., A.C., L.B., N.P., and E.S.-G. performed research; G.T., A.B.-G., F.M., P.G., G.F., and G.M. supervised research; G.T., S.A., and I.B.-D.R. analyzed data; and G.T., G.F., and G.M. wrote the manuscript. All authors edited and approved the manuscript.

DECLARATION OF INTERESTS

The authors declare no competing interests.

Received: February 15, 2019
Revised: May 23, 2019
Accepted: June 13, 2019
Published: July 18, 2019

REFERENCES

1. Smeets, M.A.M., and Dijksterhuis, G.B. (2014). Smelly primes - when olfactory primes do or do not work. Front. Psychol. *5*, 96.
2. Sullivan, R.M., Wilson, D.A., Ravel, N., and Mouly, A.-M. (2015). Olfactory memory networks: from emotional learning to social behaviors. Front. Behav. Neurosci. *9*, 36.
3. Buck, L., and Axel, R. (1991). A novel multigene family may encode odorant receptors: a molecular basis for odor recognition. Cell *65*, 175–187.
4. Ghosh, S., Larson, S.D., Hefzi, H., Marnoy, Z., Cutforth, T., Dokka, K., and Baldwin, K.K. (2011). Sensory maps in the olfactory cortex defined by long-range viral tracing of single neurons. Nature *472*, 217–220.
5. Sosulski, D.L., Bloom, M.L., Cutforth, T., Axel, R., and Datta, S.R. (2011). Distinct representations of olfactory information in different cortical centres. Nature *472*, 213–216.
6. Bekkers, J.M., and Suzuki, N. (2013). Neurons and circuits for odor processing in the piriform cortex. Trends Neurosci. *36*, 429–438.
7. Neville, K.R., and Haberly, L.B. (2004). Olfactory cortex. In The Synaptic Organization of the Brain, G.M. Shepherd, ed. (Oxford University), pp. 415–454.
8. Wilson, D.A., and Sullivan, R.M. (2011). Cortical processing of odor objects. Neuron *72*, 506–519.
9. Piomelli, D. (2003). The molecular logic of endocannabinoid signalling. Nat. Rev. Neurosci. *4*, 873–884.
10. Drumond, A., Madeira, N., and Fonseca, R. (2017). Endocannabinoid signaling and memory dynamics: A synaptic perspective. Neurobiol. Learn. Mem. *138*, 62–77.
11. Marsicano, G., and Lafenêtre, P. (2009). Roles of the endocannabinoid system in learning and memory. Curr. Top. Behav. Neurosci. *1*, 201–230.
12. Araque, A., Castillo, P.E., Manzoni, O.J., and Tonini, R. (2017). Synaptic functions of endocannabinoid signaling in health and disease. Neuropharmacology *124*, 13–24.
13. Kano, M., Ohno-Shosaku, T., Hashimotodani, Y., Uchigashima, M., and Watanabe, M. (2009). Endocannabinoid-mediated control of synaptic transmission. Physiol. Rev. *89*, 309–380.
14. Marsicano, G., and Kuner, R. (2008). Anatomical distribution of receptors, ligands and enzymes in the brain and in the spinal cord: circuitries and neurochemistry. In Cannabinoids and the Brain, A. Köfalvi, ed. (Springer), pp. 161–201.
15. Ghosh, S., Reuveni, I., Zidan, S., Lamprecht, R., and Barkai, E. (2018). Learning-induced modulation of the effect of endocannabinoids on inhibitory synaptic transmission. J. Neurophysiol. *119*, 752–760.
16. Pouille, F., and Schoppa, N.E. (2018). Cannabinoid receptors modulate excitation of an olfactory bulb local circuit by cortical feedback. Front. Cell. Neurosci. *12*, 47.
17. Soria-Gómez, E., Bellocchio, L., and Marsicano, G. (2014). New insights on food intake control by olfactory processes: the emerging role of the endocannabinoid system. Mol. Cell. Endocrinol. *397*, 59–66.
18. Soria-Gómez, E., Bellocchio, L., Reguero, L., Lepousez, G., Martin, C., Bendahmane, M., Ruehle, S., Remmers, F., Desprez, T., Matias, I., et al. (2014). The endocannabinoid system controls food intake via olfactory processes. Nat. Neurosci. *17*, 407–415.
19. Wang, Z.-J., Sun, L., and Heinbockel, T. (2012). Cannabinoid receptor-mediated regulation of neuronal activity and signaling in glomeruli of the main olfactory bulb. J. Neurosci. *32*, 8475–8479.
20. Barnes, D.C., Hofacer, R.D., Zaman, A.R., Rennaker, R.L., and Wilson, D.A. (2008). Olfactory perceptual stability and discrimination. Nat. Neurosci. *11*, 1378–1380.
21. Mediavilla, C., Martin-Signes, M., and Risco, S. (2016). Role of anterior piriform cortex in the acquisition of conditioned flavour preference. Sci. Rep. *6*, 33365.
22. Schoenbaum, G., and Eichenbaum, H. (1995). Information coding in the rodent prefrontal cortex. I. Single-neuron activity in orbitofrontal cortex compared with that in pyriform cortex. J. Neurophysiol. *74*, 733–750.
23. Rusiniak, K.W., Hankins, W.G., Garcia, J., and Brett, L.P. (1979). Flavor-illness aversions: potentiation of odor by taste in rats. Behav. Neural Biol. *25*, 1–17.
24. Slotnick, B.M., Bell, G.A., Panhuber, H., and Laing, D.G. (1997). Detection and discrimination of propionic acid after removal of its 2-DG identified major focus in the olfactory bulb: a psychophysical analysis. Brain Res. *762*, 89–96.
25. Busquets-Garcia, A., Oliveira da Cruz, J.F., Terral, G., Pagano Zottola, A.C., Soria-Gómez, E., Contini, A., Martin, H., Redon, B., Varilh, M., Ioannidou, C., et al. (2018). Hippocampal CB_1 receptors control incidental associations. Neuron *99*, 1247–1259.e7.
26. Marsicano, G., Goodenough, S., Monory, K., Hermann, H., Eder, M., Cannich, A., Azad, S.C., Cascio, M.G., Gutiérrez, S.O., van der Stelt, M., et al. (2003). CB1 cannabinoid receptors and on-demand defense against excitotoxicity. Science *302*, 84–88.

27. Monory, K., Massa, F., Egertová, M., Eder, M., Blaudzun, H., Westenbroek, R., Kelsch, W., Jacob, W., Marsch, R., Ekker, M., et al. (2006). The endocannabinoid system controls key epileptogenic circuits in the hippocampus. Neuron *51*, 455–466.
28. Busquets-Garcia, A., Soria-Gómez, E., Ferreira, G., and Marsicano, G. (2017). Representation-mediated aversion as a model to study psychotic-like states in mice. Bio Protoc. *7*, e2358.
29. Busquets-Garcia, A., Soria-Gómez, E., Redon, B., Mackenbach, Y., Vallée, M., Chaouloff, F., Varilh, M., Ferreira, G., Piazza, P.V., and Marsicano, G. (2017). Pregnenolone blocks cannabinoid-induced acute psychotic-like states in mice. Mol. Psychiatry *22*, 1594–1603.
30. Soria-Gómez, E., Busquets-Garcia, A., Hu, F., Mehidi, A., Cannich, A., Roux, L., Louit, I., Alonso, L., Wiesner, T., Georges, F., et al. (2015). Habenular CB1 receptors control the expression of aversive memories. Neuron *88*, 306–313.
31. Sevelinges, Y., Desgranges, B., and Ferreira, G. (2009). The basolateral amygdala is necessary for the encoding and the expression of odor memory. Learn. Mem. *16*, 235–242.
32. Yasoshima, Y., Morimoto, T., and Yamamoto, T. (2000). Different disruptive effects on the acquisition and expression of conditioned taste aversion by blockades of amygdalar ionotropic and metabotropic glutamatergic receptor subtypes in rats. Brain Res. *869*, 15–24.
33. Gutiérrez-Rodríguez, A., Puente, N., Elezgarai, I., Ruehle, S., Lutz, B., Reguero, L., Gerrikagoitia, I., Marsicano, G., and Grandes, P. (2017). Anatomical characterization of the cannabinoid CB_1 receptor in cell-type-specific mutant mouse rescue models. J. Comp. Neurol. *525*, 302–318.
34. Suzuki, N., and Bekkers, J.M. (2006). Neural coding by two classes of principal cells in the mouse piriform cortex. J. Neurosci. *26*, 11938–11947.
35. Suzuki, N., and Bekkers, J.M. (2011). Two layers of synaptic processing by principal neurons in piriform cortex. J. Neurosci. *31*, 2156–2166.
36. Remmers, F., Lange, M.D., Hamann, M., Ruehle, S., Pape, H.-C., and Lutz, B. (2017). Addressing sufficiency of the CB1 receptor for endocannabinoid-mediated functions through conditional genetic rescue in forebrain GABAergic neurons. Brain Struct. Funct. *222*, 3431–3452.
37. Ruehle, S., Remmers, F., Romo-Parra, H., Massa, F., Wickert, M., Wörtge, S., Häring, M., Kaiser, N., Marsicano, G., Pape, H.-C., and Lutz, B. (2013). Cannabinoid CB1 receptor in dorsal telencephalic glutamatergic neurons: distinctive sufficiency for hippocampus-dependent and amygdala-dependent synaptic and behavioral functions. J. Neurosci. *33*, 10264–10277.
38. Suzuki, N., and Bekkers, J.M. (2010). Inhibitory neurons in the anterior piriform cortex of the mouse: classification using molecular markers. J. Comp. Neurol. *518*, 1670–1687.
39. Marsicano, G., and Lutz, B. (1999). Expression of the cannabinoid receptor CB1 in distinct neuronal subpopulations in the adult mouse forebrain. Eur. J. Neurosci. *11*, 4213–4225.
40. Mazo, C., Grimaud, J., Shima, Y., Murthy, V.N., and Lau, C.G. (2017). Distinct projection patterns of different classes of layer 2 principal neurons in the olfactory cortex. Sci. Rep. *7*, 8282.
41. Haberly, L.B., and Price, J.L. (1978). Association and commissural fiber systems of the olfactory cortex of the rat. J. Comp. Neurol. *178*, 711–740.
42. Suzuki, N., and Bekkers, J.M. (2012). Microcircuits mediating feedforward and feedback synaptic inhibition in the piriform cortex. J. Neurosci. *32*, 919–931.
43. Poo, C., and Isaacson, J.S. (2009). Odor representations in olfactory cortex: "sparse" coding, global inhibition, and oscillations. Neuron *62*, 850–861.
44. Wilson, R.I., and Nicoll, R.A. (2001). Endogenous cannabinoids mediate retrograde signalling at hippocampal synapses. Nature *410*, 588–592.
45. Bellocchio, L., Lafenêtre, P., Cannich, A., Cota, D., Puente, N., Grandes, P., Chaouloff, F., Piazza, P.V., and Marsicano, G. (2010). Bimodal control of stimulated food intake by the endocannabinoid system. Nat. Neurosci. *13*, 281–283.
46. Zerucha, T., Stühmer, T., Hatch, G., Park, B.K., Long, Q., Yu, G., Gambarotta, A., Schultz, J.R., Rubenstein, J.L.R., and Ekker, M. (2000). A highly conserved enhancer in the *Dlx5/Dlx6* intergenic region is the site of cross-regulatory interactions between *Dlx* genes in the embryonic forebrain. J. Neurosci. *20*, 709–721.
47. El-Brolosy, M.A., and Stainier, D.Y.R. (2017). Genetic compensation: a phenomenon in search of mechanisms. PLoS Genet. *13*, e1006780.
48. El-Brolosy, M.A., Kontarakis, Z., Rossi, A., Kuenne, C., Günther, S., Fukuda, N., Kikhi, K., Boezio, G.L.M., Takacs, C.M., Lai, S.-L., et al. (2019). Genetic compensation triggered by mutant mRNA degradation. Nature *568*, 193–197.
49. Rossato, J.I., Moreno, A., Genzel, L., Yamasaki, M., Takeuchi, T., Canals, S., and Morris, R.G.M. (2018). Silent learning. Curr. Biol. *28*, 3508–3515.e5.
50. Choi, G.B., Stettler, D.D., Kallman, B.R., Bhaskar, S.T., Fleischmann, A., and Axel, R. (2011). Driving opposing behaviors with ensembles of piriform neurons. Cell *146*, 1004–1015.
51. Meissner-Bernard, C., Dembitskaya, Y., Venance, L., and Fleischmann, A. (2019). Encoding of odor fear memories in the mouse olfactory cortex. Curr. Biol. *29*, 367–380.e4.
52. Chapuis, J., Garcia, S., Messaoudi, B., Thevenet, M., Ferreira, G., Gervais, R., and Ravel, N. (2009). The way an odor is experienced during aversive conditioning determines the extent of the network recruited during retrieval: a multisite electrophysiological study in rats. J. Neurosci. *29*, 10287–10298.
53. Roesch, M.R., Stalnaker, T.A., and Schoenbaum, G. (2007). Associative encoding in anterior piriform cortex versus orbitofrontal cortex during odor discrimination and reversal learning. Cereb. Cortex *17*, 643–652.
54. Laviolette, S.R., and Grace, A.A. (2006). Cannabinoids potentiate emotional learning plasticity in neurons of the medial prefrontal cortex through basolateral amygdala inputs. J. Neurosci. *26*, 6458–6468.
55. Miranda, M.A., Ferry, B., and Ferreira, G. (2007). Basolateral amygdala noradrenergic activity is involved in the acquisition of conditioned odor aversion in the rat. Neurobiol. Learn. Mem. *88*, 260–263.
56. Luna, V.M., and Morozov, A. (2012). Input-specific excitation of olfactory cortex microcircuits. Front. Neural Circuits *6*, 69.
57. Hegoburu, C., Parrot, S., Ferreira, G., and Mouly, A.-M. (2014). Differential involvement of amygdala and cortical NMDA receptors activation upon encoding in odor fear memory. Learn. Mem. *21*, 651–655.
58. Wesson, D.W., and Wilson, D.A. (2011). Sniffing out the contributions of the olfactory tubercle to the sense of smell: hedonics, sensory integration, and more? Neurosci. Biobehav. Rev. *35*, 655–668.
59. Caputi, A., Melzer, S., Michael, M., and Monyer, H. (2013). The long and short of GABAergic neurons. Curr. Opin. Neurobiol. *23*, 179–186.
60. Franks, K.M., Russo, M.J., Sosulski, D.L., Mulligan, A.A., Siegelbaum, S.A., and Axel, R. (2011). Recurrent circuitry dynamically shapes the activation of piriform cortex. Neuron *72*, 49–56.
61. Reuveni, I., Lin, L., and Barkai, E. (2018). Complex-learning induced modifications in synaptic inhibition: mechanisms and functional significance. Neuroscience *381*, 105–114.
62. Zhan, C., and Luo, M. (2010). Diverse patterns of odor representation by neurons in the anterior piriform cortex of awake mice. J. Neurosci. *30*, 16662–16672.
63. Sturgill, J.F., and Isaacson, J.S. (2015). Somatostatin cells regulate sensory response fidelity via subtractive inhibition in olfactory cortex. Nat. Neurosci. *18*, 531–535.
64. Marsicano, G., Wotjak, C.T., Azad, S.C., Bisogno, T., Rammes, G., Cascio, M.G., Hermann, H., Tang, J., Hofmann, C., Zieglgänsberger, W., et al. (2002). The endogenous cannabinoid system controls extinction of aversive memories. Nature *418*, 530–534.
65. Paxinos, G., and Franklin, K.B.J. (2005). The Mouse Brain in Stereotaxic Coordinates, Fourth Edition (Academic Press).
66. Puente, N., Bonilla-Del Río, I., Achicallende, S., Nahirney, P.C., and Grandes, P. (2019). High-resolution immunoelectron microscopy techniques for revealing distinct subcellular type 1 cannabinoid receptor domains in brain. Bio Protoc. *9*, e3145.

STAR★METHODS

KEY RESOURCES TABLE

REAGENT or RESOURCE	SOURCE	IDENTIFIER
Antibodies		
Anti-Digoxigenin- Horseradish peroxidase (HRP)	Sigma- Aldrich	CAT#11207733910; RRID: AB_514500
Anti-Fluorescein-POD- Horseradish peroxidase (HRP)	Sigma-Aldrich	CAT#11426346910; RRID: AB_840257
Donkey Anti-Goat Alexa 488	Fischer Scientific	CAT#A-11055; RRID: AB_2534102
DIG riboprobes against GAD65	[39]	Riboprobes GAD65-DIG lab stock
FITC riboprobes against CB1 receptor	[39]	Riboprobes CB1-FITC lab stock
Goat polyclonal CB1 receptor	Frontier Science Co	CB1-Go-Af450-1; RRID: AB_2571592
Gold-labeled rabbit anti-goat Immunoglobulin G	Nanoprobes	CAT#2004; RRID: AB_2631182
Bacterial and Virus Strains		
AAV-CAG-GFP	[25]	Virus n°1 lab stock
AAV-CAG-CRE	[25]	Virus n°4 lab stock
Chemicals, Peptides, and Recombinant Proteins		
AM251	Tocris Bioscience	CAT#1117
Benzaldehyde	Sigma-Aldrich	CAT#418099
Cyanine 3-labeled tyramide (TSA)	Perkin Elmer	CAT#NEL744001KT
Epon resin 812:	Sigma-Aldrich	N/A
- Epoxy embedding medium (EEM), Epon 812 substitude		-CAT#45345
-EEM, hardener DDSA ($C_{16}H_{26}O_3$)		-CAT#45346
-EEM, hardener MNA ($C_{10}H_{10}O_3$)		-CAT#45347
-N-benzyldimethylamine ($C_9H_{13}N$)		-CAT#185582
FITC-conjugated tyramide (TSA)	Perkin Elmer	CAT#NEL741001KT
Glutaraldehyde	Merck Millipore	CAT#820603
HQ Silver kit	Nanoprobes	CAT#2012
Isoamyl acetate	Sigma-Aldrich	CAT#W205508
Osmium tetroxide	Electron Microscopy Sciences	CAT#19150
Pontamine sky blue	Sigma-Aldrich	CAT#C8679
Quinine hydrochloride	Sigma-Aldrich	CAT#Q1125
Reynold's lead citrate:	N/A	N/A
-Lead (II) nitrate ($(PbO_3)_2$)	-PanReac AppliChem	-CAT#131473
-Sodium hydroxide pellets (NaOH)	-Merck Millipore	-CAT#131687.1211
–3-sodium citrate 2-hydrate ($Na_3C_6H_5O_7 \cdot 2H_2O$)	N/A	-CAT#6448
Rimonabant (SR141716)	Cayman Chemical	CAT#9000484
WIN 55,212-2	Tocris Bioscience	CAT#1038
Experimental Models: Organisms/Strains		
Mouse: CB1 flox	[64]	N/A
Mouse: CB1 KO	[64]	N/A
Mouse: CB1 Rescue	[33, 36, 37]	N/A
Mouse: CB1 Stop	[33, 36, 37]	N/A
Mouse: Dlx-CB1 Rescue	[33, 36]	N/A
Mouse: Nex-CB1 Rescue	[37]	N/A
Mouse: Dlx-CB1 KO	[27, 45]	N/A
Software and Algorithms		
Adobe Photoshop	Adobe Systems	CS3
Axograph	Agrograph Software	N/A
Clampfit	Molecular devices	pClamp10

(*Continued on next page*)

Continued		
REAGENT or RESOURCE	SOURCE	IDENTIFIER
GraphPad prism 6.0	GraphPad Software	prism 6.0
ImageJ	NIH	N/A
Other		
Digidata	Molecular devices	1440 A
Electron Microscope	JEOL	JEM-1400 Plus
Epifluorescence microscope	Leica	DM6000
Guide cannulae	Bilaney	N/A
MultiClamp amplifier	Molecular devices	700B
Patch-clamp microscope	Zeiss	Axio Examiner.A1

LEAD CONTACT AND MATERIALS AVAILABILITY

This study did not generate new unique reagents. Further information and requests for resources and reagents should be directed to and will be fulfilled by the Lead Contact, Giovanni Marsicano (giovanni.marsicano@inserm.fr).

EXPERIMENTAL MODEL AND SUBJECT DETAILS

All experimental procedures were approved by the local Committee on Animal Health and Care of Bordeaux and the French Ministry of Agriculture and Forestry (authorization number A33063098) and Committee of Ethics for Animal Welfare of the University of the Basque Country (CEEA/408/2015/Grandes Moreno, CEIAB/ 213/2015/Grandes Moreno). Two to three months-old naive male *CB1-flox* [mice carrying the ''floxed'' *CB1* gene (*CB1* f/f)] were used [26, 27, 64]. Rescue, stop and knockout lines were generated as described [33, 36, 37, 64]. Briefly, Stop-CB1 mouse line was produced by silencing the endogenous *CB1* gene with a *loxP*-flanked stop cassette in the 5′ UTR of the CB1 receptor start codon. To rescue the expression of the CB_1 receptor, Stop-CB1 line was crossed with a Cre-deleter mouse line. Conditional rescue mice were obtained by crossing Stop-CB_1 mice with Dlx5/6-CRE mice (gene expressed in differentiating GABAergic neurons) allowing the expression of CB1 in GABAergic neurons, named as ''GABA-CB1 rescue,'' and with Nex-CRE mice (gene expressed in cortical glutamatergic neurons) allowing the expression of CB1 in cortical glutamatergic neurons, named as ''Glu-CB1 rescue.'' Total CB1 receptor knockout (*CB1*-KO) mice and conditional knockout animals lacking CB1 receptor in forebrain GABAergic Dlx5/6 positive neurons (GABA-*CB1*-KO) were obtained as described [27, 45, 64]. All behavioral experiments were performed during the light phase (from 9am to 1pm) and animals were kept in individual cages under a 12h light/dark cycle (lights on 7 am) and were maintained under standard conditions with food and water *ad libitum* prior undergoing behavioral procedures. At least three animals from each genotype or experimental group were used for immunohistochemistry, fluorescent *in situ* hybridization and electrophysiology recordings.

METHOD DETAILS

Behavioral procedures

Conditioned Odor Preference (COP)

Mice were water deprived during the whole protocol. During three consecutive days, animals had 1-hour access to two bottles of water. Over the following 4 days, animals received simultaneously (1-hour access) one bottle with an odor-scented solution, either banana (isoamyl acetate, 0.05%) or almond (benzaldehyde, 0.01%) diluted in water and one bottle with a different odor-scented solution (either almond or banana) mixed with the sweet taste sucrose (0.15M, 5%). Concentrations of banana (0.05%) and almond (0.01%) solutions were chosen to be equally consumed when diluted in water and prior to any associations with other stimuli [25, 28, 29]. Moreover, these almond- and banana-scented solutions were chosen to specifically served as odor cue based on previous studies indicating anosmic animals were unable to reliably detect almond- or banana-scented water (at higher concentrations than the ones used here), whereas they performed as well as control for taste detection [23, 24]. This provides evidence that these aqueous banana and almond compounds did not confer any behaviorally detected gustatory sensation to the drinking solution.

During COP training, the odor-scented solution present in water was named odor 1 (O1) and the other odor-scented solution associated with sucrose was named odor 2+Sucrose (O2+Sucrose). Half of the mice received banana-sucrose and the other half almond-sucrose. No differences were observed between either conditions in all the experiments performed. The position of the bottles was changed every day. After this training, a preference test was performed using a 1-hour two bottles choice: each bottle was presented with an odor-alone solution (almond versus banana diluted in water without sucrose). Subjects showing COP will drink more liquid in the bottle with the odor previously associated with sucrose (C+) than in the other bottle (C-).

In order to test the impact of CB1 receptor blockade in some experiments (Figures 1E, 6J, and 6K), mice injected with either the CB1 receptor antagonist (either AM251 in aPC or Rimonabant IP) or vehicle prior to the first COP test received 4 additional odor-sucrose pairings and were injected with the other treatment (either vehicle or CB1 receptor antagonist) before a second COP test.

Sucrose Preference

All subjects underwent 3 days habituation to water followed by 3 days with two bottles containing either water or sucrose. Finally, we evaluated the effect of aPC injection of AM251, or its vehicle, on their preference for sucrose over water.

Conditioned Odor Aversion (COA)

COA induced by gastric malaise. COA using gastric malaise was adapted from previous studies [25, 28–30]. Mice followed the same habituation phase as described above. The conditioning phase consisted in 4 days. On days 4 and 6 the subjects received 1-hour access to odorized water (banana or almond) followed by an injection of Saline immediately after the session (O1 + sal.). On Days 5 and 7 subjects received 1-hour access to the other odor (almond or banana) that they did not receive on Days 4 and 6, followed by an injection of lithium chloride (LiCl, 0.3 M, 1% b.w.; Sigma-Aldrich; O2 + LiCl) immediately after the session. The different odors were counterbalanced between each group. After this conditioning, the subjects were given a recovery day during which they received water dispensed in two bottles during 1 hour. The following day, a preference test was performed using a 1-hour two bottles choice: each bottle was presented with an odor (almond versus banana). During the test, subjects showing COA will drink less liquid in the bottle with the odor previously associated with LiCl (C+) than in the other bottle (C-).

COA induced by quinine. The COA with quinine followed the same procedure as the COP by replacing the sucrose by 0.1mM of quinine (Sigma-Aldrich). During the test, subjects showing COA will drink less liquid in the bottle with the odor previously associated with quinine (C+) than in the other bottle (C-). An index of preference or aversion was calculated for COP or COA experiments as the following:

$$\frac{\textbf{\textit{Liquid intake of}}\,(\boldsymbol{C}+)\;-\;\textbf{\textit{liquid intake of}}\,(\boldsymbol{C}-)}{\textbf{\textit{Total liquid intake}}}$$

Surgery

Mice were anesthetized by IP injection of a mixture of ketamine (100mg/kg, Imalgene 500) and xylazine (10mg/kg, Rompun) or with isoflurane. Then, animals were placed into a stereotaxic apparatus (Model 900, Kopf instruments, CA, USA) with a mouse adaptor and lateral ear bars. For local deletion of CB1 receptors [25, 27] in the aPC, CB1 flox mice were injected with an AAV-cag-CRE or its control AAV-cag-GFP (mixed serotype AAV1/AAV2, 10^{10} Vg/ml) into the aPC (250μl per side, 125μl/min) with the following coordinates according to Paxinos and Franklin's mouse brain atlas [65]: AP +1.6, L ± 2.5, DV −4.8. For each animal receiving AAV-cag-CRE, CB1 deletion was verified by Fluorescent *In Situ* Hybridization against CB1 mRNA. To control that recombination did not involve the posterior PC or the anterior olfactory nucleus, data were obtained by averaging CB1 mRNA fluorescence intensity from 2/4 slices for each level in the antero-posterior axis (Figures S1H and S1I). In order to check region specificity across the medio-lateral axis, data were obtained from brain regions (insular cortex, aPC and lateral olfactory tubercle) bilaterally in the section for each mouse where maximal deletion of CB1 mRNA was observed (Figure 1C). Corresponding sections were quantified in both antero-posterior and medio-lateral axes in control mice injected with AAV-cag-GFP.

For local pharmacology experiments, mice were bilaterally implanted with 3.5mm stainless steel guide cannulae (Bilaney, UK) targeting the aPC with the following coordinates [65]: AP +1.6, L ± 2.5, DV −4.5. Guide cannulae were secured in place with dental cement. Mice were allowed to recover for 2 weeks in individual cages before the beginning of the experiments.

The placement of aPC cannulae was determined by injection of 2% pontamine sky blue solution (0.5μl per side).

Drugs

For *in vitro* patch-clamp experiment, WIN 55,212-2 (5μM) (Tocris Bioscience) and AM251 (4μM) (Tocris Bioscience) were prepared in Dimethyl Sulfoxide (DMSO) and applied for 10min.

For behavioral experiments, AM251 was dissolved in a mixture of 10% Cremophor-EL, 10% DMSO and 80% saline (NaCl 0.9%). AM251 (4μg/0.5μl per side) or its vehicle was injected bilaterally in the aPC using silicone tubing connected to a peristaltic pump (PHD 22/2000 Syringe Pump Infusion, Harvard Apparatus, Massachusetts, USA, flow rate: 0.5μl/min). Rimonabant (Cayman Chemical) was dissolved in a mixture of 1.25% Tween20, 1.25% DMSO and 97.5% saline (NaCl 0.9%). Rimonabant (1 mg/kg) or its vehicle was injected intraperitoneally (IP) in a volume of 10 ml/kg.

Mice injected with AM251 (4μg/0.5μl per side) or Rimonabant (1mg/kg) were left in their home cage 10 min or 30min before bottles presentation, respectively. In order to habituate animals to receive aPC infusion and systemic injection, animals were injected with a saline solution (NaCl 0.9%) in the same manner during the two previous days. Mice receiving local aPC infusion were kept awake and maintained by the tail during the injection.

Immunohistochemistry

Mice were anesthetized with pentobarbital (Exagon, 400 mg/kg body weight), transcardially perfused with phosphate-buffered solution (PBS 0.1M, pH 7.4) before being fixed with 4% formaldehyde prepared at 4°C. Serial coronal sections were cut at 40μm and collected in PBS at room temperature (RT). Sections were permeabilized in a blocking solution of 10% donkey serum, 0.3% Triton X-100 and 0.02% sodium azide in PBS for 1 hour at RT. Free-floating sections were incubated with a goat polyclonal antibody

against C-terminal sequence of the mouse CB1 receptor (1:2000, Frontier Science) for 48h at 4°C. After several washes, slices were incubated for 2 hours with a secondary anti-goat antibody conjugated to Alexa 488 (1:500, Fisher Scientific) and then washed in PBS at RT. Finally, sections were incubated with DAPI (1:20 000, Fisher Scientific) for 5 minutes before being washed, mounted and coverslipped. The fluorescence was visualized with an epifluorescence Leica DM6000 microscope.

Immunocytochemistry for electron microscopy

For detailed methodological procedure see [66]. Coronal anterior Piriform Cortex (aPC) vibrosections were cut at 50 μm and collected in 0.1 M phosphate buffer (pH 7.4) at RT. Sections were preincubated in a blocking solution of 10% BSA, 0.1% sodium azide, and 0.02% saponin prepared in 1X Tris-HCl-buffered saline, pH 7.4, for 30 minutes at RT. A pre-embedding silver-intensified immunogold method was used for localization of the CB1 receptor protein. Briefly, aPC sections were incubated with the primary goat polyclonal anti-CB_1 receptor antibody (2 μg/ml Frontier Sciences Institute; goat polyclonal) in 10% BSA/Tris-HCl-buffered saline containing 0.1% sodium azide and 0.004% saponin on a shaker for 48h at 4°C. After several washes in 1% BSA/Tris-HCl-buffered saline, tissue sections were incubated with a secondary 1.4-nm gold-labeled rabbit anti-goat Immunoglobulin G (Fab fragment; 1:100; Nanoprobes) in 1% BSA/Tris-HCl-buffered saline with 0.004% saponin on a shaker for 4 hours at RT. Sections were washed in 1% BSA/ Tris-HCl-buffered saline overnight at 4°C and postfixed in 1% glutaraldehyde in Tris-HCl-buffered saline for 10 minutes at RT. After several washes in double-distilled water, gold particles were silver intensified with an HQ Silver kit (Nanoprobes Inc.) for approximately 12 minutes in the dark and then washed in double-distilled water first, and in a 0.1M phosphate buffer, pH 7.4 later. Stained sections were osmicated (1% osmium tetroxide, in 0.1 M phosphate buffer, pH 7.4, 20 minutes), dehydrated in graded alcohols to propylene oxide, and plastic-embedded in Epon resin 812. Ultrathin sections of 50 nm were collected on nickel mesh grids, stained with 2.5% lead citrate for 20 minutes, and examined in a JEOL JEM 1400 Plus electron microscope. Tissue preparations were photographed by using a digital camera coupled to the electron microscope. Adjustments in contrast and brightness were made to the figures in Adobe Photoshop (Adobe Systems, San Jose, CA).

Fluorescent *in situ* hybridization

The procedure was performed as described [18, 39]. Briefly, mice were sacrificed by cervical dislocation. Their brains were extracted, frozen on dry ice and stored at −80°C until sectioning in a cryostat (14 μm, Microm HM 500M, Microm Microtech). Fluorescein (FITC)-labeled riboprobes against mouse CB1 receptor and digoxigenin (DIG)-labeled riboprobes against mouse GAD65 were prepared as described [39]. After hybridization overnight at 60°C with the mixture of probes, the slides were washed with different stringency wash buffers at 65°C. Then, the slides were blocked with a blocking buffer prepared according to the manufacturer's protocol. Anti-DIG or anti-FITC antibodies conjugated to horseradish peroxidase (HRP) (Roche; 1:2000) were applied 2 hours at RT or overnight at 4°C to detect respectively GAD65-DIG or CB1-FITC probes. Probes hybridization was revealed by a tyramide signal amplification (TSA) reaction using Cyanine 3-labeled tyramide (Perkin Elmer; 1:100 for 10 minutes) to detect GAD65 signal or FITC-conjugated tyramide (Perkin Elmer; 1:80 for 12 minutes) to amplify the signal of CB1. The slides were incubated in 4',6-diamidino-2-phenylindole (DAPI; 1:20 000; FISHER Scientific) before being washed, coverslipped and visualized with an epifluorescence Leica DM6000 microscope.

Electrophysiology

All the animals were sacrificed by dislocation during the light phase (9am to 12am). The brains were quickly removed and immerged in ice-cold oxygenated cutting solution containing in mM: 180 Sucrose, 26 $NaHCO_3$, 12 $MgCl_2$, 11 Glucose, 2.5 KCl, 1.25 NaH_2PO_4, 0.2 $CaCl_2$, oxygenated with 95% O2/5% CO_2 ≈300mOsm. Coronal aPC slices (300μm thick) were obtained using a vibratome (VT1200S, Leica) and transferred for 30min into a 34°C bath of oxygenated ACSF containing in mM: 123 NaCl, 26 $NaHCO_3$, 11 Glucose, 2.5 KCl, 2.5 $CaCl_2$, 1.3 $MgCl_2$, 1.25 NaH_2PO_4 ≈305 mOsm. After a minimum of 30min recovery at RT (22-25°C), slices were transferred to a recording chamber in ACSF at 32°C. Recordings were performed using a Multiclamp 700B amplifier (Molecular devices) in principal glutamatergic neurons clamped with glass pipettes (3-5 MΩ) filled with an internal solution containing in mM: 130 KCl, 10 HEPES, 1 EGTA, 2 $MgCl_2$, 0.3 $CaCl_2$, 7 Phosphocreatin, 3 Mg-ATP, 0.3 Na-GTP; pH = 7.2; 290mOsm. These cells were identified based on their morphology and somatic location using a contrast microscope (axio examiner.A1, Zeiss) and through electrical properties by measuring their resting potential and their excitability in current-clamp mode after 300ms steps of current injections from −50 to 300pA with steps of 25pA [34, 35, 51]. Neurons with large apical dendrites, soma located in the upper half of layer II, resting potential of around −70mV, input resistance of around 200-300 MΩ and displaying regular spiking were considered as semilunar-like cells (SL; Figures S5A and S5B). Instead, neurons with large basal dendrites, soma located in the lower half of layer II and upper part of layer III, resting potential around −75mV, input resistance of around 100-150 MΩ and showing initial burst firing were classified as pyramidal-like neurons (PN; Figures S5A and S5B). Given the complex layered structure of the aPC, miniature inhibitory post-synaptic currents (mIPSCs), known to be regulated by CB1 receptors [44], were specifically chosen to avoid restricting the study of inhibitory inputs coming from a specific layer where the stimulating electrode would have been placed. mIPSCs were obtained in voltage clamp mode in presence of NMDA and AMPA/Kainate receptor antagonists (50μM D-APV and 10μM NBQX) and of the voltage-gated sodium channels blocker, tetrodotoxin (1μM TTX). Vehicle (DMSO) was applied before starting the recording and CB1 agonist (WIN 5μM) and antagonist (AM251 4μM) were applied for 10min successively. For experiments performed after behavior, animals underwent the two bottles choice test for 15min and were sacrificed 5min later. mIPSCs were collected in the same manner as for naive animals, for 5 min in presence of vehicle (DMSO).

QUANTIFICATION AND STATISTICAL ANALYSIS

Behavioral data

For all the experiments, data are presented as absolute liquid intake. Considering the variability of liquid consumption during the two first days of pairings (likely due to the random choice of a bottle at day 1 and the confusion that might appear because of the inverted position of the bottles at day 2), only the last two days of the learning phase showing a reliable preference/aversion behavior were presented for each experiments.

Numerical evaluation for electron microscopy

Semiquantitative analysis of CB1 receptor presence in excitatory or inhibitory terminals was done in aPC layers I and II of *CB1*-WT and *CB1*-KO according to our published procedure [66]. Total analyzed area was more than 2200 μm^2 per genotype (n = 3).

Numerical evaluation for FISH

Cells expressing mRNAs were quantified in the three layers of the aPC. Because CB1 mRNA level is variable, CB1 positive cells were classified according to the level of transcript visualized by the intensity of fluorescence [39]. "High-CB1" cells were considered to be round-shaped and intense staining covering the entire nucleus whereas "Low-CB1" cells were defined with discontinuous shape and lowest intensity of fluorescence allowing the discrimination of grains of staining. Numerical evaluation of the double FISH was performed manually in 118 sections from 4 animals, by evaluating the coexpression of CB1-positive cells with GAD 65 marker.

Electrophysiology

Electrophysiological data were filtered at 4kHz by a Digidata 1440A (Molecular devices) and they were collected during the last 5min of recording in each condition. Electrical properties were analyzed with Clampfit and mIPSCs were analyzed using Axograph software.

Statistics

Electrophysiological and behavioral data were analyzed with Prism Software (GraphPad). Repeated or unpaired statistical analyses were obtained with Student's t test,ANOVA (one-way or two way), mixed effects analysis and linear regression to compare two or multiple groups and for correlation where appropriate. When ANOVA provided significant main factor effects or significant interactions, Dunnett or Sidak post hoc analyses were performed as appropriate. Statistical details are presented in Tables S1, S2, and S3. Significance was set at $p < 0.05$ and data are expressed as mean ± SEM.

DATA AND CODE AVAILABILITY

This study did not generate datasets/code. Further data information are available upon request by contacting the Lead Contact, Giovanni Marsicano (giovanni.marsicano@inserm.fr).

Current Biology, Volume *29*

Supplemental Information

CB1 Receptors in the Anterior Piriform Cortex Control Odor Preference Memory

Geoffrey Terral, Arnau Busquets-Garcia, Marjorie Varilh, Svein Achicallende, Astrid Cannich, Luigi Bellocchio, Itziar Bonilla-Del Río, Federico Massa, Nagore Puente, Edgar Soria-Gomez, Pedro Grandes, Guillaume Ferreira, and Giovanni Marsicano

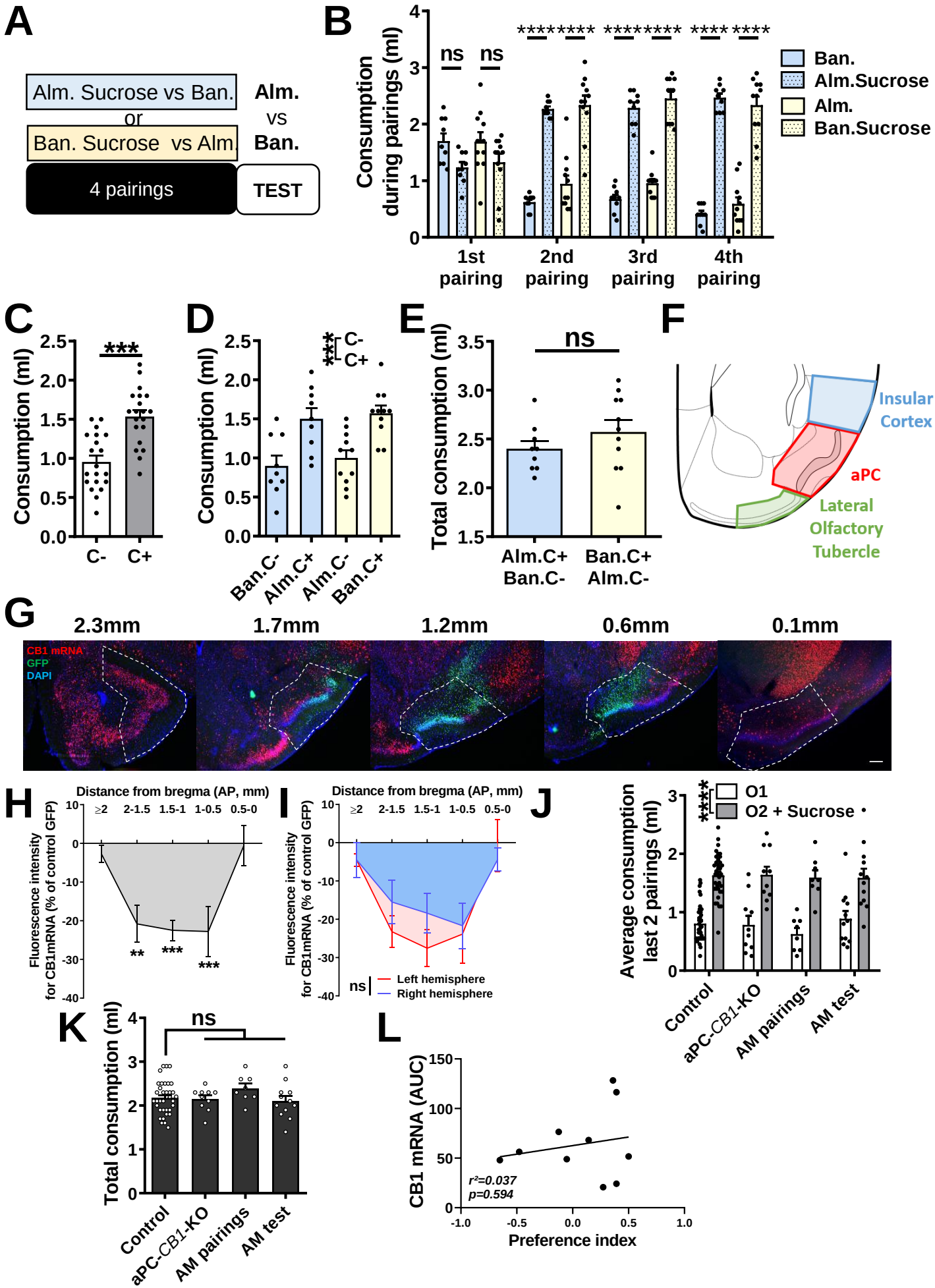
A
Alm. Sucrose vs Ban.
or
Ban. Sucrose vs Alm.
4 pairings
TEST
Alm.
vs
Ban.
B
Consumption during pairings (ml)
ns
ns
****
****
****
****
Ban.
Alm.Sucrose
Alm.
Ban.Sucrose
1st pairing
2nd pairing
3rd pairing
4th pairing
C
Consumption (ml)
***
C-
C+
D
Consumption (ml)
***
C-
C+
Ban.C-
Alm.C+
Alm.C-
Ban.C+
E
Total consumption (ml)
ns
Alm.C+ Ban.C-
Ban.C+ Alm.C-
F
Insular Cortex
aPC
Lateral Olfactory Tubercle
G
2.3mm
1.7mm
1.2mm
0.6mm
0.1mm
CB1 mRNA
GFP
DAPI
H
Distance from bregma (AP, mm)
≥2
2-1.5
1.5-1
1-0.5
0.5-0
Fluorescence intensity for CB1mRNA (% of control GFP)
**
***
***
I
Distance from bregma (AP, mm)
Fluorescence intensity for CB1mRNA (% of control GFP)
ns
Left hemisphere
Right hemisphere
J
Average consumption last 2 pairings (ml)
***
O1
O2 + Sucrose
Control
aPC-CB1-KO
AM pairings
AM test
K
Total consumption (ml)
ns
Control
aPC-CB1-KO
AM pairings
AM test
L
CB1 mRNA (AUC)
r²=0.037
p=0.594
Preference index

Figure S1. CB1 receptors in the aPC are necessary for the retrieval of conditioned odor preference. Related to Figure 1

(A) Schematic representation of the protocol used for conditioned odor preference (COP). **(B)** Consumption of the almond- and banana-scented solutions during sucrose conditioning (Ban. Alm.Sucrose, n=9; Alm. Ban.Sucrose, n=11). **(C)** COP test consumption of the odor-scented solutions previously associated with sucrose (C+) or not (C-; n=20). **(D)** Consumption of C+ and C- during the COP test depending on the odor-scented solution used as C+ (Almond C+ in blue or Banana C+ in yellow). **(E)** Total liquid consumption during the COP test. **(F)** Representative areas used to analyze fluorescence intensity of FISH for CB1 mRNA in *CB1-flox* mice infused with AAV-GFP or AAV-Cre into the aPC. **(G)** Representative images along the antero-posterior axis of the aPC in a *CB1-flox* mouse that received AAV-Cre virus into the aPC. FISH against CB1mRNA (red), immunostaining for GFP (green) and DAPI (blue). **(H-I)** Average between both hemispheres **(H)** or within each hemisphere **(I)** of the fluorescence intensity for CB1 mRNA along the antero-posterior axis of the aPC from *CB1-flox* mice infused with AAV-Cre virus (n=10) as compared with AAV-GFP control mice (n=7) used in COP experiments. **(J)** Average consumption during the last two days of training in the different groups (control, n=36; aPC-*CB1*-KO, n=10; AM pairings, n=8 and AM test, n=12). **(K)** Total liquid consumption during the test in the different groups (control, aPC-*CB1*-KO, AM pairings and AM test). **(L)** Correlation between the average deletion of CB1 mRNA in the antero-posterior axis (area under the curve, AUC, corresponding to H) of mice infused with AAV-Cre and their COP retrieval performance (n=10). **, $p<0.01$; ***, $p<0.001$; ****, $p<0.0001$; ns, not significant. For statistical details, see Table S2.

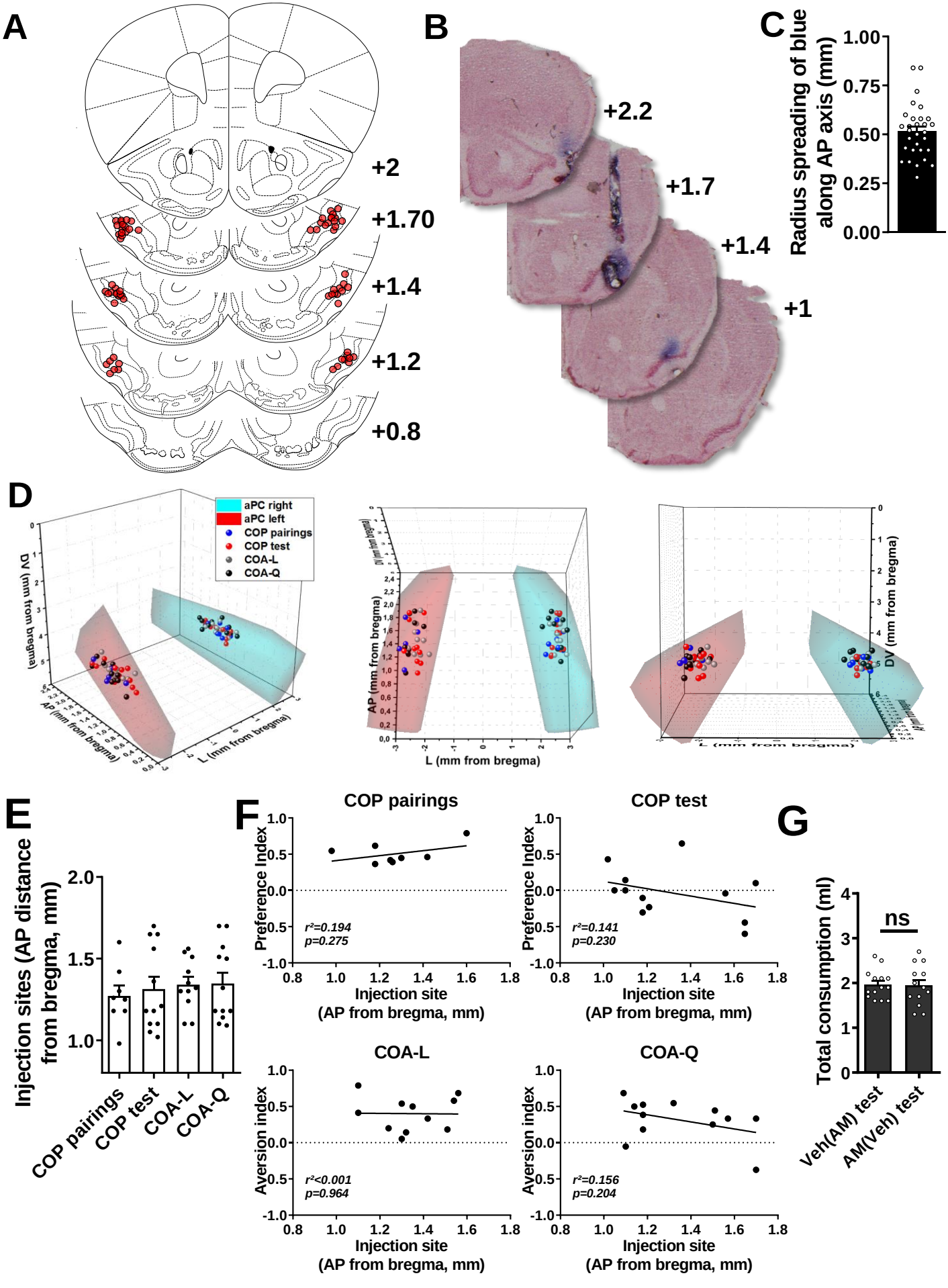
A
+2
+1.70
+1.4
+1.2
+0.8
B
+2.2
+1.7
+1.4
+1
C
Radius spreading of blue along AP axis (mm)
1.00
0.75
0.50
0.25
0.00
D
aPC right
aPC left
COP pairings
COP test
COA-L
COA-Q
DV (mm from bregma)
AP (mm from bregma)
L (mm from bregma)
E
Injection sites (AP distance from bregma, mm)
2.0
1.5
1.0
COP pairings
COP test
COA-L
COA-Q
F
COP pairings
COP test
COA-L
COA-Q
Preference Index
Aversion index
r²=0.194
p=0.275
r²=0.141
p=0.230
r²<0.001
p=0.964
r²=0.156
p=0.204
Injection site
(AP from bregma, mm)
G
Total consumption (ml)
ns
Veh(AM) test
AM(Veh) test

Figure S2. CB1 receptors in the aPC are necessary for the retrieval of conditioned odor preference. Related to Figures 1 & 2

(A) Injection cannula tips in the aPC of 35 randomly selected vehicle or AM251 treated mice from all the pharmacological experiments (red circles). Adapted from Paxinos and Watson [65]. **(B)** Representative image showing the aPC injected site (blue) for local pharmacological treatments. Numbers in **(A)** and **(B)** indicate the relative position of coronal slices from bregma. **(C)** Radius spreading along the antero-posterior axis of the pontamine sky blue injected through 30 cannula randomly selected from the different pharmacological experiments. **(D)** Three-dimensional representation of the cannula-injected sites of AM251 treated animals in the different pharmacological experiments performed in the study (COP pairings, n=8; COP test, n=12; COA-L, n=11 and COA-Q, n=12). **(E)** Mean antero-posterior sites of injection of AM251 treated animals for all pharmacological experiments. **(F)** Correlation between the behavioral performance (preference or aversion index) and the antero-posterior sites of AM251 injection for each pharmacological study. **(G)** Total liquid consumption during the test day in animals performing the second test after retraining [Veh(AM) test, n=14; AM(Veh) test, n=13]. *, $p<0.05$; **, $p<0.01$; ***, $p<0.001$; ****, $p<0.0001$; ns, not significant. For statistical details, see Table S2.

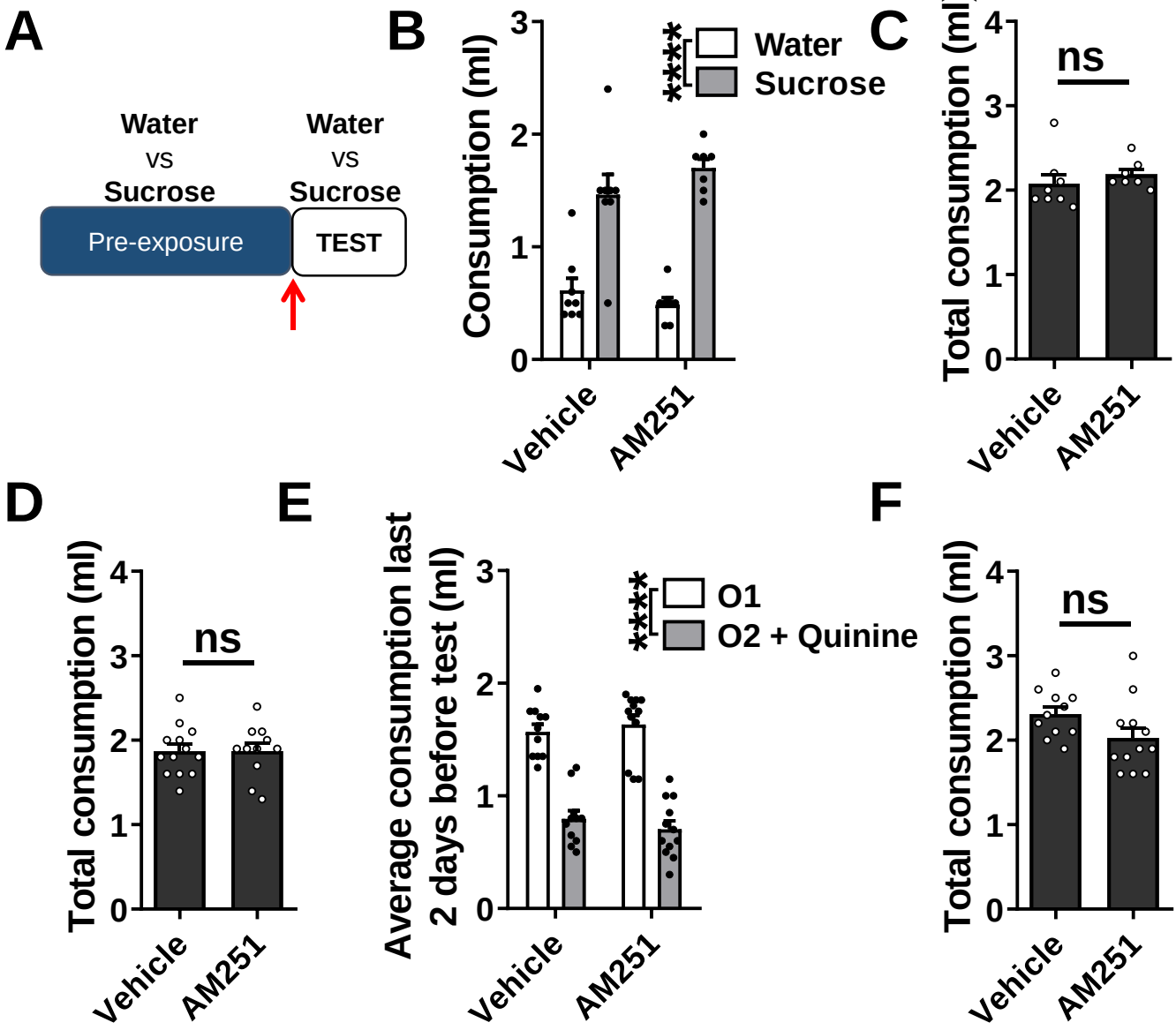

Figure S3. CB1 receptors in the aPC are not involved in sucrose preference nor in the retrieval of conditioned odor aversion. Related to Figure 2

(A) Schematic representation of the protocol used to evaluate the effect of aPC infusion (red arrow) of the CB1 receptor antagonist AM251 (4µg/0.5µl) or Vehicle on spontaneous sucrose preference. **(B)** Consumption of sucrose solution and water after aPC infusion of Vehicle (n=8) or AM251 (n=7) during the sucrose preference test. **(C)** Total liquid consumption during the sucrose preference test. **(D)** Total liquid consumption during the retrieval test of COA-L (Vehicle, n=13; AM251, n=11). **(E)** Average consumption during the last two days of training COA-Q of the odor-scented solutions paired with quinine (O2 + Quinine) or not (O1; Vehicle, n=11; AM251, n=13). **(F)** Total liquid consumption during retrieval test of COA-Q. ****, p<0.0001; ns, not significant. For statistical details, see Table S3.

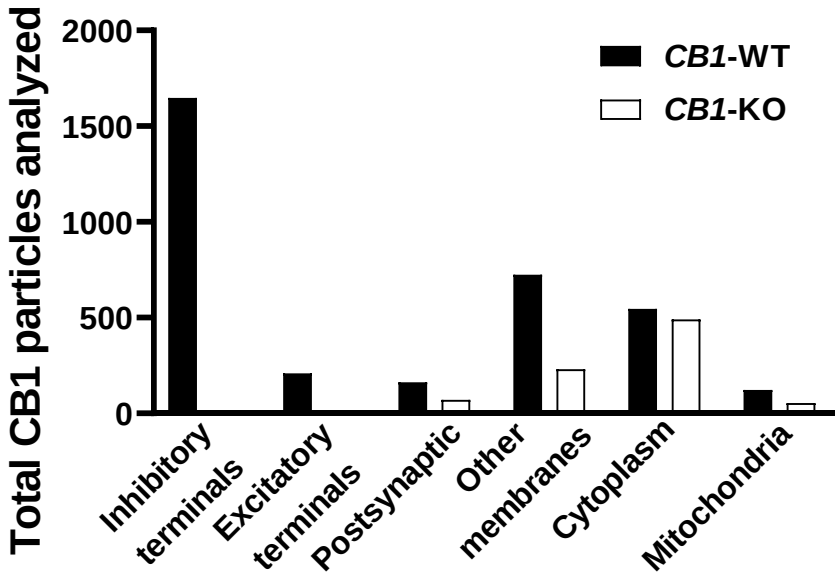

Figure S4. CB1 receptors are highly expressed in inhibitory terminals in the aPC. Related to Figure 3

Total CB1 receptor immunoparticles analyzed in different cellular compartments (Inhibitory terminals, Excitatory terminals, Postsynaptic, Other membranes, Cytoplasm and Mitochondria) in *CB1*-WT and *CB1*-KO mice (n=3 per genotype).

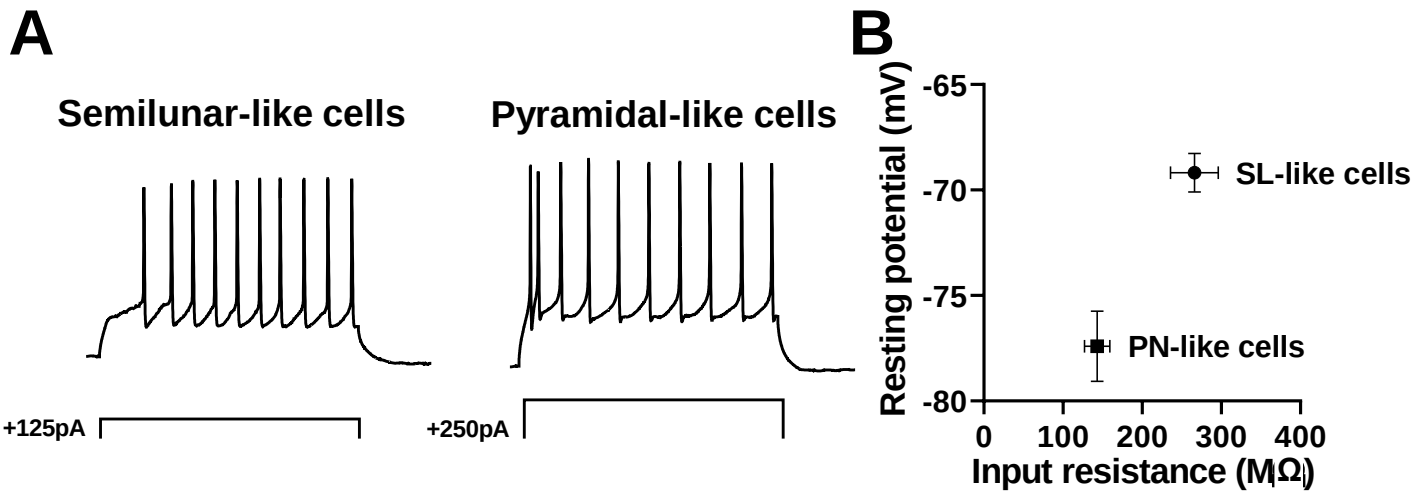

Figure S5. Physiological properties of aPC principal neurons. Related to Figures 5 & 6

(A) Representative spiking pattern of semilunar-like neurons (SL, left) and of pyramidal-like neurons (PNs, right) in response to current injection (SL, 125pA for 300ms; PNs, 250pA for 300ms). **(B)** Resting potential and input resistance characteristics recorded from SL cells and PNs in Figure 5 (SL, n=10; PN, n=9).

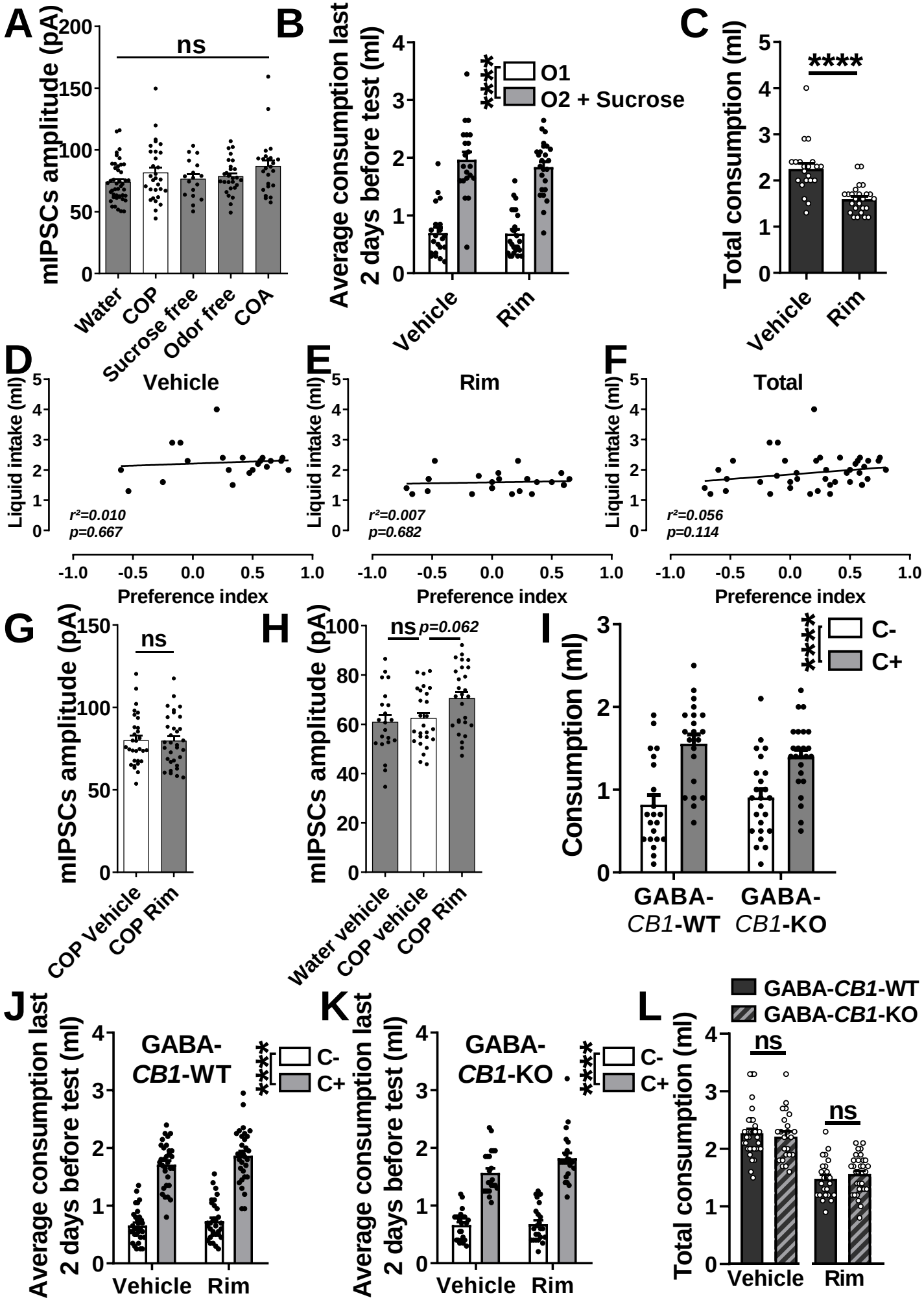
A
mIPSCs amplitude (pA)
ns
Water
COP
Sucrose free
Odor free
COA
B
Average consumption last 2 days before test (ml)
****
O1
O2 + Sucrose
Vehicle
Rim
C
Total consumption (ml)
****
Vehicle
Rim
D
Vehicle
Liquid intake (ml)
r²=0.010
p=0.667
Preference index
E
Rim
r²=0.007
p=0.682
F
Total
r²=0.056
p=0.114
G
mIPSCs amplitude (pA)
ns
COP Vehicle
COP Rim
H
mIPSCs amplitude (pA)
ns
p=0.062
Water vehicle
COP vehicle
COP Rim
I
Consumption (ml)
****
C-
C+
GABA-CB1-WT
GABA-CB1-KO
J
GABA-CB1-WT
Average consumption last 2 days before test (ml)
****
C-
C+
Vehicle
Rim
K
GABA-CB1-KO
L
GABA-CB1-WT
GABA-CB1-KO
Total consumption (ml)
ns
ns

Figure S6. COP retrieval is associated with CB1 receptor-dependent modulation of inhibitory transmission on specific aPC principal cells. Related to Figure 6

(A) Quantifications of mIPSCs amplitude recorded in SL neurons from mice sacrificed during water consumption (Water, n=44 cells from 10 animals), COP retrieval test (COP, n=30 from 8 animals), exposure to odor-scented solutions without sucrose (Sucrose free, n=17 cells from 4 animals), exposure to sucrose solution without odors (Odor free, n= 27 cells from 4 animals), or COA retrieval test (COA, n= 24 cells from 4 animals). **(B)** Average consumption during the last two days of training of the odor-scented solutions paired with sucrose (O2 + Sucrose) or not (O1; Vehicle, n=21; Rim, n=25). (**C**) Total liquid consumption during the COP test in animals injected IP with either vehicle or the CB1 antagonist Rimonabant (Rim, 1 mg/kg). **(D-F)** Correlation between the liquid intake during the test and COP retrieval performance in mice receiving systemic injection of **(D)** Vehicle (n=21), **(E)** Rim (n=25) and **(F)** in both treatment condition (Total, n=46). **(G)** Quantification of mIPSCs amplitude recorded in SL neurons from mice sacrificed during COP retrieval test and treated with Vehicle (COP Vehicle, n=30 cells from 5 animals) or Rim (COP Rim, n=32 cells from 5 animals). **(H)** Quantification of mIPSCs amplitude recorded in PNs from mice sacrificed during water consumption (Water vehicle, n=21 from 3 animals) or COP retrieval test and treated with Vehicle (COP vehicle, n=26 cells from 4 animals) or Rim (COP Rim, n=27 cells from 5 animals). **(I)** Consumption of the odor-scented solutions (C+ and C-) during test of COP in GABA-*CB1*-KO mice (n=24) and their WT littermates (GABA-*CB1*-WT, n=21). **(J)** Average consumption during the last two days of training in GABA-*CB1*-WT mice (n=31). **(K)** Average consumption during the last two days of training in GABA-*CB1*-KO mice (n=23). **(L)** Total liquid consumption during the test in GABA-*CB1*-WT and GABA-*CB1*-KO mice treated with vehicle and Rim. ****: $p<0.0001$; ns, not significant. For statistical details, see Table S3.

Figure	Conditions	n	Analysis (post hoc)	Factors analyzed	F-ratios	P values
1C	Fluorescence intensity for CB1 mRNA	7-10	Unpaired t-test	CRE vs GFP	Insular cortex t=0.1280 df=15	P = 0.8998
					aPC t=4.964 df=15	P = 0.0002
					Lat. Olf. Tub. t= 0.2985 df=15	P = 0.7694
1D	COP in aPC-*CB1*-KO mice and AM251-treated mice	36-10-8-12	Two-way ANOVA repeated measures (Sidak)	Control vs KO treatment	Interaction, F (3,62) = 5.919	P = 0.0013
				C+ vs C-	control	P < 0.0001
					aPC-CB1-KO	P = 0.8902
					AM pairings	P < 0.0001
					AM test	P > 0.9999
1E	COP in AM251-treated mice (reverse experiment)	12-13	Two-way ANOVA repeated measures (Sidak)	Vehicle vs AM251	Interaction, F (1,25) = 7.913	P = 0.0165
				C+ vs C-	Veh(AM) test	P = 0.0029
					AM(Veh) test	P = 0.9993
2B	COA-L in AM251-treated mice	13-11	Two-way ANOVA repeated measures	Vehicle vs AM251 C+ vs C-	Interaction, F (1,22) = 0.066	P = 0.8002
					Solution, F (1,22) = 34.73	P < 0.0001
2D	COA-Q in AM251-treated mice	11-12	Two-way ANOVA repeated measures	Vehicle vs AM251 C+ vs C-	Interaction, F (1,21) = 2.032	P = 0.1687
					Solution, F (1,21) = 52.25	P < 0.0001
3C	Distribution CB1 particles	9	Unpaired t-test	Inhibitory vs Excitatory	t=21.60 df=16	P < 0.0001
3D	Proportion of CB1 particles at terminals	9	Unpaired t-test	WT vs KO: Inhibitory	t=117.1 df=16	P < 0.0001
				WT vs KO: Excitatory	t=14.87 df=16	P < 0.0001
5B	Effect of WIN on mIPSCs frequency of WT mice – SL	10	One-way ANOVA repeated measures (Dunnett)	Vehicle vs drugs	F (2, 18) = 15.33	P = 0.0001
					Vehicle vs WIN	P = 0.0126
					Vehicle vs WIN+AM251	P = 0.1107
5C	Effect of WIN on mIPSCs amplitude of WT mice – SL	10	One-way ANOVA repeated measures (Dunnett)	Vehicle vs drugs	F (2, 18) = 5.365	P = 0.0223
					Vehicle vs WIN	P = 0.0569
					Vehicle vs WIN+AM251	P = 0.0701
5E	Effect of WIN on mIPSCs frequency of WT mice – PN	9	One-way ANOVA repeated measures	Vehicle vs drugs	F (2, 16) = 2.366	P = 0.1395
5F	Effect of WIN on mIPSCs amplitude of WT mice – PN	9	One-way ANOVA repeated measures	Vehicle vs drugs	F (2, 16) = 0.9548	P = 0.3844
6B	mIPSCs frequency after behaviors – SL	44-30-17-27-24	One-way ANOVA (Dunnett)	Water vs conditions	F (4,137) = 4.181	P = 0.0032
					Water vs COP	P = 0.0031
6C	COP in mice treated with rimonabant IP	21-25	Two-way ANOVA repeated measures	Vehicle vs Rim	Interaction, F (1,44) = 6.420	P = 0.0149
				C+ vs C-	Vehicle	P = 0.0005
					Rim	P = 0.8163
6E	mIPSCs frequency in COP-Rim treated mice – SL	30-32	Unpaired t-test	Vehicle vs Rim	t=2.340 df=60	P = 0.0227
6F	Correlation SL frequency over preference index	10	Linear Regression analysis	Frequency vs preference index	Linear fit	$r^2 = 0.4272$
					Slope, F (1,8)	P = 0.0404
6H	mIPSCs frequency after behaviors – PN	21-26-27-	One-way ANOVA (Dunnett)	COP vehicle vs conditions	F (2,71) = 5.742	P = 0.0049
					Water veh vs COP veh	P = 0.0073
					COP veh vs COP Rim	P = 0.9446
6I	Correlation PN frequency over preference index	9	Linear Regression analysis	Frequency vs preference index	Linear fit	$r^2 = 0.2964$
					Slope, F (1,7)	P = 0.1297
6J	COP in GABA-CB1-WT mice treated IP with vehicle and Rimonabant	31	Two-way ANOVA repeated both factors (Sidak)	Vehicle vs Rim	Interaction, F (1,30) = 3.894	P = 0.0577
				C+ vs C-	Vehicle	P = 0.0010
					Rim	P = 0.4717
6K	COP in GABA-CB1-KO mice treated IP with vehicle and Rimonabant	23	Two-way ANOVA repeated both factors	Vehicle vs Rim C+ vs C-	Interaction, F (1,22) = 0.2405	P = 0.6287
					Solution, F (1,22) = 19.27	P = 0.0002

Table S1. Statistical analysis. Related to Figures 1-3 & 5,6

Figure	Conditions	n	Analysis (post hoc)	Factors analyzed	F-ratios	P values
S1B	Consumption during pairings for COP in WT mice	9-11	Two-way ANOVA repeated measures (Sidak)	Banana vs Almond	Interaction, F (7,72) = 21.90	P < 0.0001
				C+ vs C-	C+ vs C-, F (1,72) = 238.6	P < 0.0001
S1C	COP total consumption in WT mice	20	Paired t-test	C+ vs C-	t=4.120 df=19	P = 0.0006
S1D	COP for almond and banana in WT mice	9-11	Two-way ANOVA repeated measures	Banana vs Almond C+ vs C-	Interaction, F (1,18) = 0.0091	P = 0.9253
					Solution, F (1,18) = 16.74	P = 0.0007
S1E	COP total consumption for almond and banana in WT mice	9-11	Unpaired t-test	Banana vs Almond	t=1.130 df=18	P = 0.2733
S1H	Fluorescence intensity for CB1 mRNA over AP axis	10	Mixed-effects analysis	AP distance	Interaction, F (4,23) = 4.616	P = 0.0070
				CRE vs GFP	≥2	P = 0.9883
					2-1.5	P = 0.0014
					1.5-1	P = 0.0002
					1-0.5	P = 0.0003
					0.5-0	P = 0.9970
S1I	Fluorescence intensitry for CB1 mRNA deletion in CRE mice	10	Mixed-effects analysis	AP distance Left vs Right	Interaction, F (4,31)=0.6262	P = 0.6474
S1J	Average consumption during the last 2 pairings in aPC-*CB1*-KO mice and AM251-treated mice	36-10-8-12	Two-way ANOVA repeated measures	Control vs KO/treatment C+ vs C-	Interaction, F (3,62) = 0.2345	P = 0.8720
					Solution, F (1,62) = 64.87	P < 0.0001
S1K	COP total consumption in aPC-*CB1*-KO mice and AM251-treated mice	36-10-8-12	One-way ANOVA	Control vs conditions	F (3,62) = 1.123	P = 0.3467
S1L	Correlation CB1 mRNA deletion over preference index	10	Linear Regression analysis	CB1 mRNA vs preference	Linear fit	r^2 = 0.0372
					Slope, F (1,8)	P = 0.5935
S2E	AP injection sites of AM treated animals in all experiments	8-12-11-12	One-way ANOVA	Experiments	F (3,39) = 0.2347	P = 0.8716
S2F	Correlation preference index over AP injection sites	8-12-11-12	Linear Regression analysis	Preference vs AP	COP pairings: Linear fit Slope, F (1,6)	r^2 = 0.1935 P = 0.2754
					COP test: Linear fit Slope, F (1,10)	r^2 = 0.1406 P = 0.2298
					COA-L: Linear fit Slope, F (1,9)	r^2 = 0.0022 P = 0.9639
					COA-L: Linear fit Slope, F (1,10)	r^2 = 0.1560 P = 0.2038
S2G	COP total consumption in AM251-treated mice (reverse experiment)	14-13	Unpaired t-test	Vehicle vs AM251	t=0.1204 df=25	P = 0.9052

Table S2. Statistical analysis. Related to Figures 1-3 & S1, S2.

Figure	Conditions	n	Analysis (post hoc)	Factors analyzed	F-ratios	P values
S3B	Sucrose preference in AM251-treated mice	8-7	Two-way ANOVA repeated measures	Vehicle vs AM251 sucrose vs water	Interaction, F (1,13) = 1.302	P = 0.2745
					Solution, F (1,13) = 41.79	P < 0.0001
S3C	Sucrose preference total consumption in AM251-treated mice	8-7	Unpaired t-test	Vehicle vs AM251	t=0.8205 df=13	P = 0.4267
S3D	COA-L total consumption in AM251-treated mice	13-11	Unpaired t-test	Vehicle vs AM251	t=0.0281 df=22	P = 0.9778
S3E	Average consumption during the last 2 pairings in COA-Q	11-12	Two-way ANOVA repeated measures	Vehicle vs AM251 C+ vs C-	Interaction, F (1,21) = 0.6386	P = 0.4332
					Solution, F (1,21) = 75.57	P < 0.0001
S3F	COA-Q total consumption in AM251-treated mice	11-12	Unpaired t-test	Vehicle vs AM251	t=1.867 df=21	P = 0.0760
S6A	mIPSCs amplitude after behaviors	44-30-17-27-24	One-way ANOVA	Water vs conditions	F (4,137) = 2.088	P = 0.0857
S6B	Average consumption during the last 2 pairings before the test of COP with rimonabant IP	21-25	Two-way ANOVA repeated measures	Vehicle vs Rim C+ vs C-	Interaction, F (1,44) = 0.2165	P = 0.6440
					Solution, F (1,44) = 41.79	P < 0.0001
S6C	COP total consumption in mice treated with rimonabant IP	21-25	Unpaired t-test	Vehicle vs Rim	t=5.036 df=44	P < 0.0001
S6D	Correlation liquid intake over preference index in vehicle treated mice	21	Linear Regression analysis	Liquid intake vs preference	Linear fit	r^2 = 0.0100
					Slope, F (1,19)	P = 0.1918
S6E	Correlation liquid intake over preference index in rimonabant treated mice	25	Linear Regression analysis	Liquid intake vs preference	Linear fit	r^2 = 0.0074
					Slope, F (1,23)	P = 0.6818
S6F	Correlation liquid intake over preference index in all the mice treated IP	46	Linear Regression analysis	Liquid intake vs preference	Linear fit	r^2 = 0.0559
					Slope, F (1,44)	P = 0.1135
S6G	mIPSCs amplitude in COP-Rim treated mice – SL	30-32	Unpaired t-test	Vehicle vs Rim	t=0.0610 df=60	P = 0.9519
S6H	mIPSCs amplitude in COP-Rim treated mice – PN	30-32	One-way ANOVA	COP vehicle vs conditions	F (2,71) = 4.126	P = 0.0202
					Water veh vs COP veh	P = 0.9112
					COP veh vs COP Rim	P = 0.0619
S6I	COP in GABA-CB1-KO mice	21-24	Two-way ANOVA repeated both factors	Vehicle vs Rim C+ vs C-	Interaction, F (1,43) = 0.8172	P = 0.3710
					Solution, F (1,43) = 20.35	P < 0.0001
S6J	Average consumption during the last 2 pairings before the test in GABA-CB1-WT	31	Two-way ANOVA repeated both factors	Vehicle vs Rim C+ vs C-	Interaction, F (1,30) = 0.2806	P = 0.6002
					Solution, F (1,30) = 128.9	P < 0.0001
S6K	Average consumption during the last 2 pairings before the test in GABA-CB1-KO	23	Two-way ANOVA repeated both factors	Vehicle vs Rim C+ vs C-	Interaction, F (1,22) = 3.196	P = 0.0876
					Solution, F (1,22) = 90.40	P < 0.0001
S6L	Total consumption in GABA-CB1-WT and –KO during tests	31-23	Unpaired t-test	WT vs KO	Vehicle, t=0.4792 df=52	P = 0.6338
					Rim, t=0.8887 df=52	P = 0.3782

Table S3. Statistical analysis. Related to Figures 1-3, 6 & S3, S5.